Design study for the ITER polarimetry diagnostic

EFDA Technology Workprogramme 2002

Combined final report for
deliverable 5 of EFDA Contracts EFDA/01-649 (amended) (FOM),
deliverable 2/4.1 of EFDA Contract 02-1000 (ENEA-RFX)
and
deliverable 3/4.2 of EFDA Contract 02-1003 (CEA)

July 2005

A.J.H. Donné,[1] M.F. Graswinckel,[1] L. Giudicotti,[2] C. Nyhan,[2] S. L. Prunty,[3] C. Gil,[4] V.S. Voitsenya,[5] A.F. Bardamid,[6] V.N. Bondarenko,[5] V.G. Konovalov,[5] D.I. Naidenkova,[5] I.V. Ryzhkov,[5] A.N. Shapoval,[5] A.F. Shtan',[5] S.I. Solodovchenko,[5] K.I. Yakimov[6]

[1]*FOM-Institute for Plasma Physics Rijnhuizen, Association EURATOM-FOM, Partner in the Trilateral Euregio Cluster, PO Box 1207, 3430 BE Nieuwegein, The netherlands*
[2]*IGI, Consorzio RFX, Association EURATOM-ENEA, Corso Stati Uniti 4, Padova, Italy*
[3]*University College Cork, Association EURATOM-DCU, Cork, Ireland*
[4]*CEA Cadarache, DRFC/SCCP, Association EURATOM-CEA, 13108 Saint Paul les Durance Cedx, France*
[5]NSC KIPT, 61108 Kharkov, Ukraine
[6]Taras Shevchenko National University, Kiev, Ukraine

Introduction

The workpackage on the ITER poloidal polarimeter system under EFDA Technology Workprogramme 2002 was carried out by the authors from a consortium of various associations. The work was distributed under three EFDA article-5.1b contracts: one under the responsibility of CEA, one under that of IGI (ENEA-RFX), with University College Cork as subcontractor, and the other one under the responsibility of FOM, with NSC KIPT Kharkov as subcontractor. FOM acted as coordinator for the various contracts.

The reports on the subtasks are annexed. The FOM contribution consists of two parts: a design analysis of critical components (Annex I) and measurements of the reflectance of mirrors composing a corner-cube reflector (Annex II). ENEA-RFX made an experimental test of a single-chord ITER-like polarimeter configuration (Annex III), while CEA studied experimentally the effects of plasma exposure of a corner-cube reflector (Annex IV). A closely related task, optical characterization (in particular of polarization) in the FIR range of exposed mirrors, has been conducted under EFDA task TW3-TPDS-DIADEV deliverable 2 (ENEA-RFX) and is reported separately.

Deliverables

The original deliverables were:

EFDA/01-649 (FOM)

1. Resolve remaining design issues associated with the conceptual design developed during the study of earlier EFDA contracts, in particular assess the compatibility of the in-vessel optics with the ITER port plug. Apart from the retro-reflector, the issues to be considered here are the possibility to have a transmission line with only two focussing components per line, of which one (the second mirror) is placed inside the port plug. Furthermore, it should be investigated whether or not it is possible to have an automatic alignment procedure to direct the laser beam onto the retro-reflector by a mirror that is positioned as far as possible from the plasma. Finally, a conceptual design of a double vacuum barrier should be made. Since similar problems are expected for all individual polarimeter chords, it is sufficient to address those for one typical chord only.
2. Identify critical optical components and perform initial design study of these critical components, in particular the high field side retro-reflectors. Specific laboratory tests should be done to check the reflective properties of retro-reflectors after having been exposed to deuterium ions from a plasma source.
3. Perform a design study of the alignment and calibration methodologies for initial installation and during subsequent operation. Specifically one should study the tolerable angular and lateral misalignments of the various optical components to see whether these are realistic. Furthermore, it should be investigated which optical components would be the most ideal to be used as scanning mirrors.
4. Identify critical optical components and perform initial design study of these critical components, in particular the high field side retro-reflectors. Specific laboratory tests should be done to check the reflective properties of retro-reflectors after having been exposed to deuterium ions from a plasma source.

EFDA/02-1000 (ENEA-RFX)

1. Experimental tests of a single chord FIR polarimeter in conditions as similar as possible to those expected in ITER.

EFDA/02-1003 (CEA)

1. Characterize the change of optical performance of a corner-cube reflector exposed to plasma.
2. Interpret the observed changes in the optical performance in terms of plasma processes occurring at the reflecting surfaces.

As an additional contribution to the polarimeter feasibility study, research was done on semi-reflective plates, that need to be employed to split and recombine the FIR beams.

Main results

The various participants of the polarimeter consortium have addressed the points mentioned above. The work has been distributed in such a way that individual scientists have taken the lead in one or more aspects of the study. The results of the individual

studies are described in detail in the Annexes. Here only the main conclusions will be mentioned and compared to the task deliverables. The conclusions are grouped per contract.

EFDA/01-649 (FOM)

Gaussian beam raytracing calculations have been done for a typical chord of the equatorial port polarimeter system. The calculations have been done with the GRT3D code. As a starting point for the study we used the result from an earlier EFDA study that, given the 37 mm diameter of the retro-reflector, the optimum diameter for the beam waist at the retro-reflector is 13 mm. Furthermore, we have specifically followed the suggestion of previous studies to have as small as possible a number of focussing elements.

It has indeed been concluded that a rather straightforward optical system, featuring two spherical mirrors along with a set of plane mirrors is sufficient to transport the beam from laser to retro-reflector and back. One spherical mirror is positioned in the port plug (actually it is the second mirror), the other spherical mirror is positioned just inside the diagnostic laboratory. It is envisaged that a substantial part of the system can be made self-aligning with articulated transmission lines. The mirrors should be mounted in the beam line within an angular tolerance of 0.01 rad and a transverse position tolerance of 1 mm.

To cope with displacements of the beam at the retro-reflector due to e.g. refraction, movements of machine components, it is important to have a scanning option. A scan over an area of 10×10 cm^2 at the position of the retro-reflector can be achieved either by a using a mirror inside the interspace block (advantage: smaller mirrors are needed in the port and, hence, smaller neutron streaming through the port; drawback: scanning mirror not easily accessible for maintenance), or by a mirror in the access cell (with opposite advantages and drawbacks). So if, during operation of the polarimeter, a particular beam misses, for whatever reason, the retro-reflector, then that specific chord can be switched from measurement mode to scan mode. As soon as the beam is back onto the reflector the chord is again included in the measurements.

Two different cases have been studied: one with a focal length of the first spherical mirror of 4430 mm, and one with a focal length of 5100 mm. The first option has been optimised such that the dimensions of the optical elements inside the port plug and interspace block are as small as possible. However, in the access cell the beam then quickly expands. In the last 5 meters of the line, the beam does not fit in the reference design transmission lines, which have a 150 mm inner diameter. The second option has been optimised to have the smallest possible beam waist in the access cell. This option is fully compatible with the diameter of the transmission lines in the access cell. However, now the dimensions inside the port plug and interspace block are somewhat larger leading to a somewhat higher neutron streaming. Future polarimeter design work should address this issue in detail and provide an adequate answer.

A suitable design for the double window has been developed and has been accepted by the ITER safety group. It is believed that the polarimeter can be calibrated between consecutive plasma discharges. The measured polarization rotation without plasma is the cumulative effect of polarization rotation on/in the various optical components. Whether this technique is feasible depends very much on which polarimetry technique is ultimately used and therefore needs to be addressed in a forthcoming study.

It should be noted that all conclusions are based on calculations for a single line of sight. Although it is expected that the problems and solutions are similar also for other lines of sight, specific calculations need to be done to check this. For instance the distance between the retro-reflector and focussing mirror is not the same for different chords, and hence the conclusions might be slightly different for the full system.

The surface roughness of cube-corner reflectors can have a large effect on their reflective properties. In this report the reflective properties of a cube corner reflector are studied at two different wavelengths, 10.6 and 118.8 μm, which are both relevant for interferometry/ polarimetry diagnostics envisaged for ITER. The sputtering expected in ITER is simulated by bombardment of the cube-corner reflectors with deuterium ions from a plasma source. Various materials for the reflectors have been studied. One of the conclusions is that if the cube-corner reflectors envisaged for the poloidal polarimeter system in ITER (118.8 μm) are made of polycrystalline molybdenum they will maintain good reflective properties during the full ITER life cycle. This cannot be concluded for the reflectors in the toroidal polarimeter system (10.6 μm), where extensive precautions are required to reduce the sputtering by charge exchange atoms.

EFDA/02-1000 (ENEA-RFX)

FIR polarimetry in conditions of ITER has been experimentally demonstrated. A polarization modulated far-infrared (118.8 μm) input beam has been transmitted along a 31-m long optical beam line, including a corner cube retro-reflector, and used for a simultaneous measurement of Faraday rotation and Cotton Mouton effects produced by a wave-plate plasma simulator. A time resolution of 10 ms and an angular resolution equal or better than 1 degree have been demonstrated. Double pass use of the beam line was unfortunately not possible due to limits of the beam line design and lack of alignment tools for the back-reflected beam.

EFDA/02-1003 (CEA)

The surface changes of a CuCrZr corner cube mirror, which has been exposed to plasma and wall conditioning during one year were studied:

a) In the inner half a deposit was found of a not yet analysed material.

b) In the outer region, evidence for erosion was found, not following the magnetic lines.

The cumulated plasma duration was 7 hours with an average density of $2\text{-}4\times10^{19}$ m^{-3} and the total wall conditioning lasted 1000 hours.

The measured reflectivity of the retro-reflector at 118 μm showed a slight decrease (<10%). No measurable decrease was measured for plane mirrors that were also exposed.

A study of semi-reflective plates led to the conclusion that the angle of the plates must be as small as possible to minimize errors between the reflectivity for perpendicular and parallel polarisation.

Recommendations

The recommendations from the various subtasks are:

EFDA/01-649 (FOM)

1. Gaussian raytracing calculations should be done for the full optical system to check whether the main conclusions from this study also hold for other lines of sight.
2. In close conjunction with the ITER International Team it should be assessed which of the two scanning approaches (e.g by a mirror inside the interspace block or by a mirror in the access cell) is to be preferred.
3. After definition of the optical design of the full system (task 1) and the choice which scanning approach is to be preferred, one has a good overview of the diameters and geometry of all port penetrations. At this stage detailed neutronics calculations should be performed to check whether or not the neutron screening is acceptable.
4. After the technical implementation of the system has been developed, further assessment of the possible calibration options should be made and tested experimentally.
5. Recommendations on retroreflectors:
   a. Simulation experiments (using Cu mirror samples) indicate that sputtering of the top 5 μm layer from a polycrystalline metal mirror would not result in a noticeable decrease of reflectance at λ = 118.8 μm. Thus, polycrystalline molybdenum, for which sputtering over the ITER lifetime is expected to be less than 5 μm, can be recommended as material for fabrication of retro-reflectors for this specific plasma diagnostic.
   b. For the toroidal polarimetry system operating at much shorter wavelengths (λ = 10.8 μm) a similar rate of sputtering is absolutely inadmissible. This is also because the path length of the probing beam is much longer than that of the poloidal polarimetry system. Therefore, the divergence of the reflected beam would play a more serious role. To avoid this, the geometry of the holes in (or behind) which the Mo retro-reflectors are mounted, have to provide an attenuation of the CXA flux to the CCR surface by more than an order of magnitude as compared to that at the first wall flux.
   c. It was found that under bombardment by deuterium ions from a plasma, the optical properties of an imperfect single crystalline Mo mirror degrade almost as fast as the optical properties of polycrystalline mirror. It follows from this fact that due to the high degree of mechanical treatment needed for fabrication of retro-reflectors, the CCR samples fabricated from single crystalline material would loose those advantages. However, as can be concluded from results presented above, for sub-mm methods of diagnostics CCR fabricated of polycrystalline molybdenum are expected to have reasonable reflective properties during the full ITER life time.

EFDA/02-1000 (ENEA-RFX)

1. The feasibility of the polarimetric scheme foreseen for ITER has been confirmed. Further work for the definition of the design requires the selection of a specific polarimetric method and polarization modulation scheme.

EFDA/02-1003 (CEA)

1. As the change of reflectivity that has been measured is small, a more precise experiment is needed to confirm these results, and to study, under more ITER relevant FIR beam conditions, the possible change of polarisation and broadening of the Gaussian beam.
2. In order to understand the mechanisms of erosion and deposition, it would be interesting to compare the exposed mirrors with ones that are only exposed to wall conditioning. Comparisons with retro-reflectors made of others materials that have a lower erosion rate than CuCrZr such as W and Mo (mono- or poly-crystalline) is recommended.

Annex I (FOM): Critical issues in the design of the ITER polarimeter diagnostic
Annex II (FOM/Kharkov): Measurements of the reflectance of mirrors composing a corner-cube reflector
Annex III (ENEA-RFX): Experimental test of a single-chord ITER-like polarimeter configuration
Annex IV (CEA): Experimental test of plasma exposure of a corner-cube reflector

Annex I (FOM): Critical issues in the design of the ITER polarimeter diagnostic

Support to ITER Diagnostic Design
Contract: EFDA 01.649
Task:

Polarimetry
(deliverable D5)

By A.J.H. Donné and M.F. Graswinckel

December 2003

FOM Institute for Plasma Physics Rijnhuizen
Association EURATOM – FOM, Trilateral Euregio Cluster
3430 BE Nieuwegein, The Netherlands

Introduction

The aim of the polarimetry task is to address the following issues:

1. Resolve remaining design issues associated with the conceptual design developed during the study of earlier EFDA contracts[i], in particular assess the compatibility of the in-vessel optics with the ITER port plug.
2. Identify critical optical components and perform initial design study of these critical components, in particular the high field side retro-reflectors.
3. Perform design study of the alignment and calibration methodologies for initial installation and during subsequent operation.
4. Co-ordinate design activities, within the participating EU fusion associations, for the development of the system design for the ITER polarimetry diagnostic.
5. Assist the ITER IT in the updating of ITER documentation.
6. Assist the ITER IT in the updating of diagnostic cost estimates.

The conclusion of the earlier EFDA contracts was that a poloidal polarimeter seems to be a feasible instrument for measuring the current density profile in ITER. The main conclusions from this earlier study were:

1. The optimum wavelength of the system is in the range 50 – 100 μm. The choice was made for 118 μm because of the availability of strong FIR lasers operating at this wavelength. A wavelength of 57 μm was chosen as a possible fall back. Although powerful lasers are available at the latter wavelength, the needed tolerance of optical components becomes more stringent.
2. The poloidal polarimeter system consists of an equatorial fan of 10 chords with retro-reflectors mounted at approximately 25 cm indentation in the remote-handling grips of the blanket modules at the high-field side. The maximum permitted diameter of the retro-reflectors is 37 mm.
3. Additional a fan of chords via the upper port has been considered to give a higher accuracy in the region where q_{min} is expected.
4. The Faraday rotation angles and the Cotton-Mouton effect have been calculated for all chords and for a number of different density profiles and ITER equilibria. The conclusion is that the Faraday rotation angles that can be expected are large and easy to measure. Also the Cotton-Mouton effect will be large and should be taken into account. In fact the Cotton-Mouton effect is so large that it can be used as an independent density measurement.
5. Equilibrium reconstructions using simulated diagnostic signals using a database of almost 2000 different ITER equilibria have learned that the poloidal polarimeter system will drastically improve the q-profile reconstruction in the plasma centre compared with reconstruction with magnetics data only. The addition of the upper port polarimeter system gives a further – but rather marginal improvement – of the measurement accuracy.
6. The effect of refraction in the plasma has been calculated. The largest refraction effects occur for the chords looking down from the upper port, with displacement at the position of the retro-

reflectors of up to 1 cm. The effects for the equatorial fan of chords are less (up to 8 mm). The differences between plasmas with different density profiles (peaked and flat) are generally even less.

7. Simulation of the reflective properties of retro-reflectors have learned that it is advantageous to use retro-reflectors that are elongated in the poloidal direction (e.g. a toroidal width of 37 mm with a poloidal width of 60 mm). This guarantees good reflection of the beam even when it is misalignment due to refraction or whatever other cause.
8. Relative straight forward gaussian beam calculations have led to the conclusion that it must be possible to transport the beam over the full distance from the diagnostic laboratory to the tokamak and back by using only two focussing mirrors along with many flat mirrors.
9. A first analysis of the power losses in such a system of mirrors has led to the conclusion that the source power needed is achievable.

As a next step of the above study it was thought important to make a full gaussian-beam raytracing calculation for a single polarimeter chord to study various remaining design issues and to obtain a better idea of the number of optical elements needed along with the required optical tolerances.

The geometry of the ITER poloidal polarimeter system

As starting point for the raytracing calculations described in this report we have chosen to use one of the chords of the polarimeter system as was described in ref. i (see Fig. 1). The coordinates of the retro-reflector, port plug penetration as well as those of first and second mirrors are indicated in the table, inserted in Fig. 1. The second mirror is a focussing mirror.; the first one is a plane mirror. Fig. 2 shows the port plug in somewhat more detail. The first mirror reflects the beam out of the plane of the drawing (alternating to the backward and forward direction). The second mirror reflects the beam in to a plane parallel to the plane of drawing.

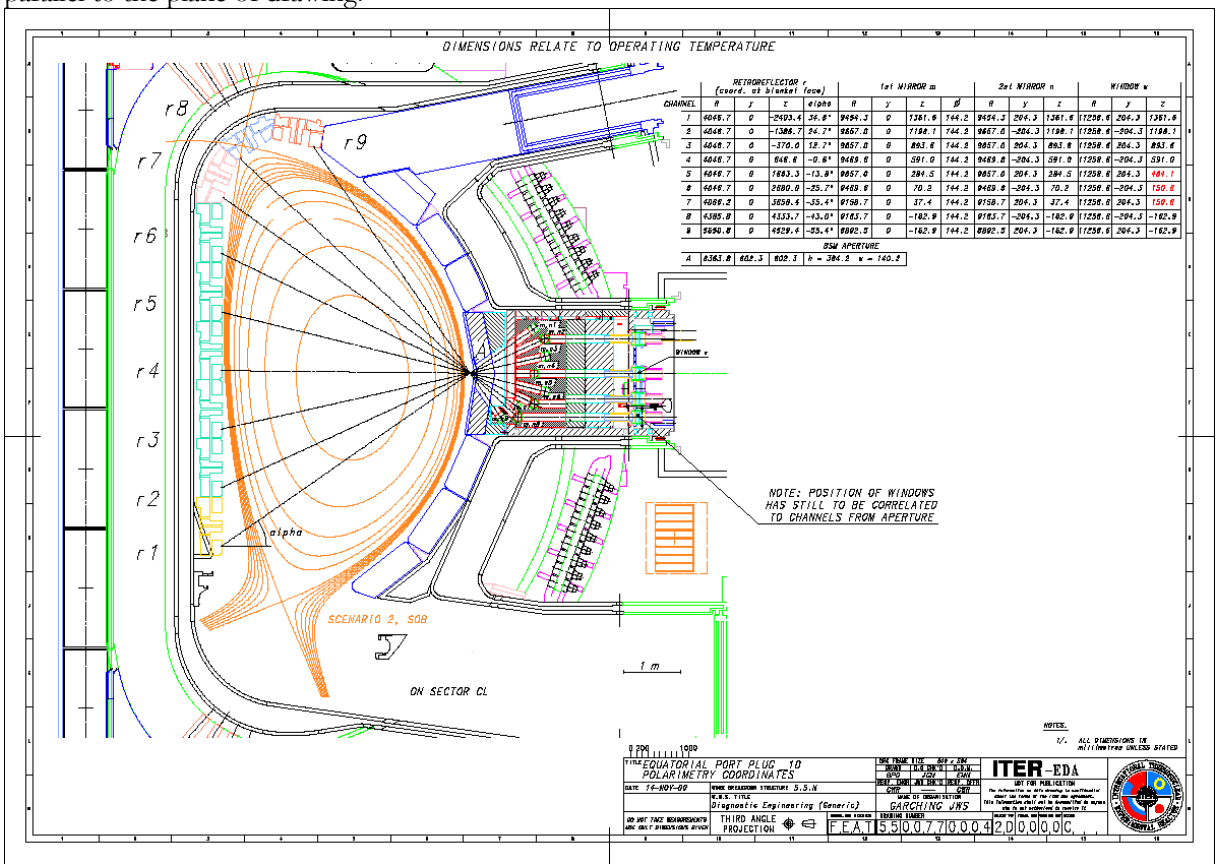

Fig. 1. Lay-out of the equatorial fan of chords of the poloidal polarimeter system for ITER. The coordinates in the inserted Table are given in relative port coordinates. R is the major radius, z is the vertical position and y is the 'toroidal' position, measured perpendicular to the R, z plane (the y-coordinate of the retro-reflector is defined to be at y = 0).

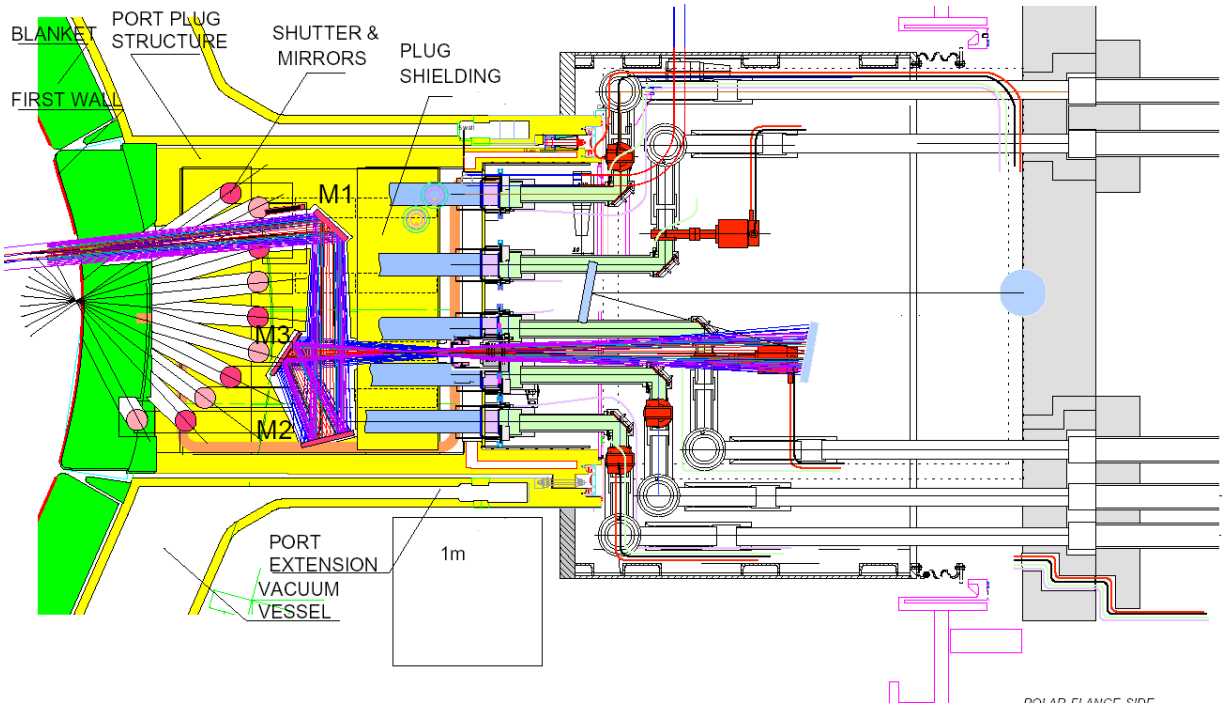

Fig. 2. Close up of the equatorial port plug. Also the rays of the LIDAR Thomson scattering system (dark blue) are indicated.

A choice was made to perform the ray-tracing calculations for chord number 5, which is the one that is probing just above the midplane. For the definition of the remaining beamline (after the second mirror) we have used the coordinates that were kindly made available to us by Chris Walker of the ITER International Team in Garching (see Table 1). A figure of the full optical system after the second mirror is shown in Figure 3. The coordinates in Table 1 are in absolute coordinates. These differ from the port coordinates by the fact that the y-coordinate is different. The x- and z-coordinates in the absolute system are similar to the R- and z-coordinates in the port coordinate system. To combine the coordinates of retro-reflector, first and second mirror, with those of the remaining optical system (after the second mirror), a coordinate transformation should be applied to one of the two systems. The position of the first vacuum window is indicated both in the Table in Figure 1 (the three right most columns) as well as in Table 1 below (PT409). The difference in window coordinates between these two Tables defines the coordinate transformation needed. The resulting coordinates are given in Table 2.

Table 1. Coordinates of the various mirrors constituting polarimeter chord #5

	X	Y	Z
*PT409	-11004.93932	-1733.32069	482.00000
*PT411	-12598.61673	-2014.32902	482.00000
*PT412	-12598.61673	-2014.32902	1154.00000
*PT413	-12773.30680	-1023.61242	1154.00000
*PT414	-17640.85693	-1881.89284	1154.00000
*PT415	-17640.85693	-1881.89284	2862.50000
*PT416	-17403.25021	-2695.49163	2862.50000
*PT417	-33250.00000	-7323.44134	2862.50000

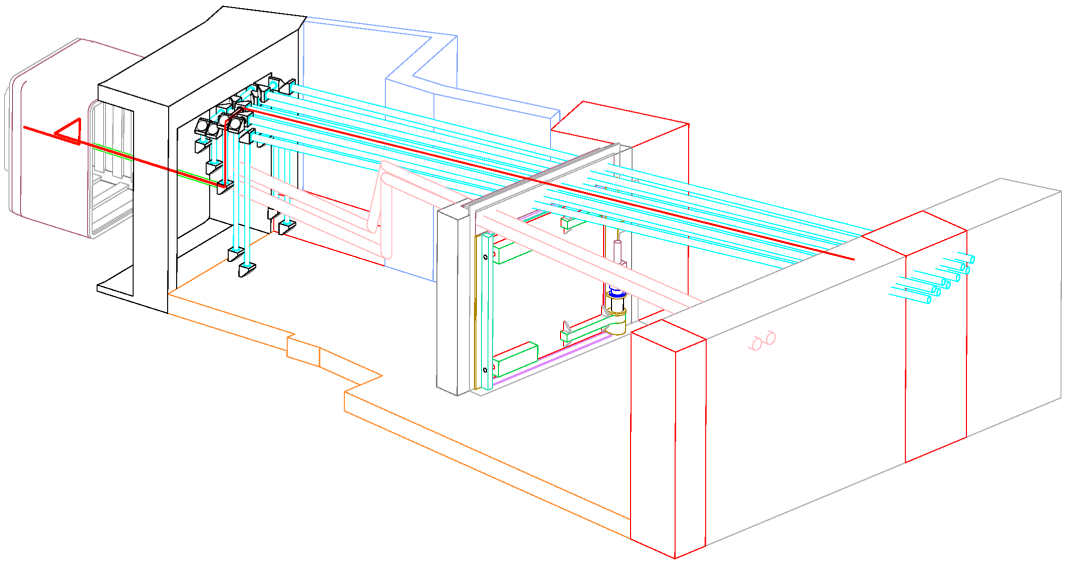

Fig. 3. Overview of the optical transmission line from the position of the first vacuum window (PT409 in Table 1) to the point of entrance into the diagnostic laboratory (PT417).

Gaussian-beam ray-tracing calculations

The gaussian-beam ray-tracing calculations have been performed with the computer program GRT3D, that was originally developed for the design of the interferometer system at the H-1NF heliac.[ii] The program has been kindly made available to us by its authors John Howard and George Warr.

Starting point of the calculations was the conclusion of the previous study,[i] namely that the optimum beam waist at the position of the retro-reflector is 13 mm diameter (or as is further used in this report a beam radius of 6.5 mm). The calculated beam waist as a function of distance in the system is indicated in Fig. 4. The red line defines the beam radius at any point in space. The vertical green lines indicate the positions of the various mirrors in the system. The following focal lengths have been used: f_{PT408} = 4430 mm and f_{PT417} = 6731 mm. The focal length of PT408 has been chosen such, that the beam radius inside the port plug and interspace block is as small as possible. This is advantageous, since it gives the possibilities to use smaller diameters of beam penetrations in the port plug, with the beneficial effect of a reduced neutron streaming. Fig. 4 (and also Fig. 5) are reversible for the in- and outgoing beams as long as the beam is well aligned on the optical axis of the system.

Table 2. Coordinates of all optical elements in the beam line of polarimeter chord # 5.

Number	Element	X (mm)	Y (mm)	Z (mm)	Focal length (mm)	Cumulative distance (mm)
PT406	Retro-reflector	-4048.70	-1937.62	1803.30		0.00
PT407	Plane mirror	-9057.60	-1937.62	284.50		5234.10
PT408	Spherical mirror	-9057.60	-1733.32	284.50	4430.00	5438.40
PT409	First window	-11004.94	-1733.32	482.00		7395.73
PT411	Plane mirror	-12598.62	-2014.33	482.00		9014.00
	Second window	-12598.62	-2014.33	818.00		9350.00
PT412	Plane mirror	-12598.62	-2014.33	1154.00		9686.00
PT413	Plane mirror	-12773.31	-1023.61	1154.00		10692.00
PT414	Plane mirror	-17640.86	-1881.89	1154.00		15634.64
PT415	Plane mirror	-17640.86	-1881.89	2862.50		17343.14
PT416	Plane mirror	-17403.25	-2695.49	2862.50		18190.73
PT417	Spherical mirror	-33250.00	-7323.44	2862.50	6731.00	34699.43

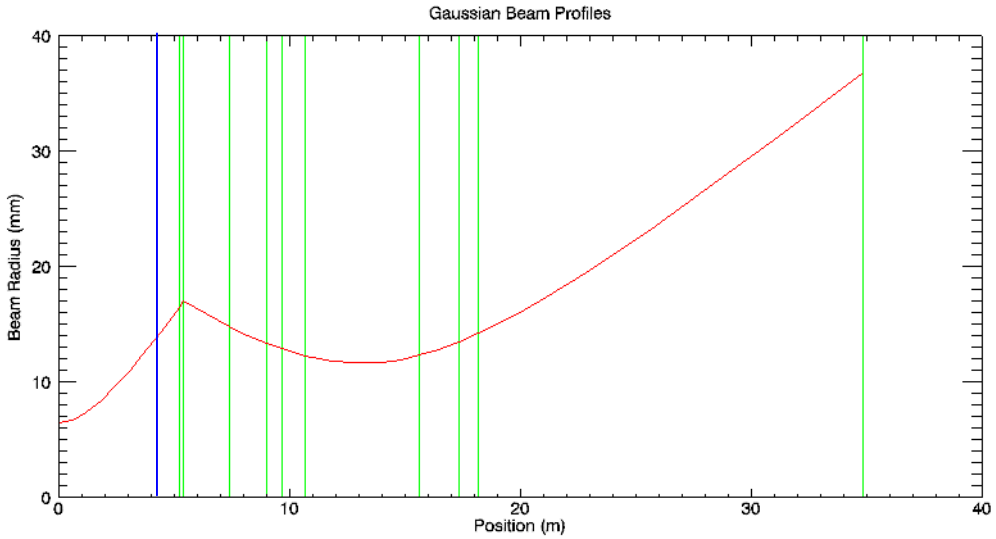

Fig. 4. Calculated waist (defined in terms of radius) of the full optical system from retro-reflector up to the second focussing mirror, close to the entrance to the laser laboratory (f_{PT408} = 4430 mm, f_{PT417} =6731 mm). The green vertical lines show the locations of the optical components. The blue line refers to the position of the port penetration.

If one would have an ideal alignment of the beam on the optical axis of the system, one could as a rule of thumb define the diameter of each optical element (as well as the diameter of beam penetrations) as a factor of 4.4 times the calculated beam radius.[iii] So in principle, this would imply that all optical elements from port penetration up to mirror PT416 could be 75 mm diameter or less. However, as we shall see further in this report, larger diameter will be needed to tolerate a certain degree of misalignments as well as to have the possibility to actively scan the beam over the retro-reflector for alignment purposes. A drawback of this relatively short focal length for PT408 is that the beam expands quickly between mirrors PT416 and PT417, from a radius of 14 mm to 37 mm. This implies a diameter of mirror PT417 of 162.8 mm (without tolerance for misalignment). This is in conflict (but only for the last 5 meter of the beam line) with the design value of the inner diameter of the transmission lines in the access cell (having 150 mm diameter). However, since the discrepancy occurs in the very last 5 meters of the beam path before it enters the diagnostic laboratory, it must be relatively straightforward to taper to somewhat larger diameter transmission lines in the last part of the access cell.

To study whether this can be optimised also calculations were performed for different focal lengths of the two focussing mirrors. A longer focal length of mirror PT408 (5100 mm instead of 4430 mm), was chosen such that the diameter of the beam at PT417 is as small as possible. The result is that a transmission line with a diameter of 140 mm over its full length can be used (see Fig. 5). However, this has as a drawback that the minimum dimensions of the elements in the interspace area become somewhat larger per individual element. Nevertheless, not accounting for any misalignments a diameter of 75 mm for the full in-port and interspace optics and beam diameter is still enough.

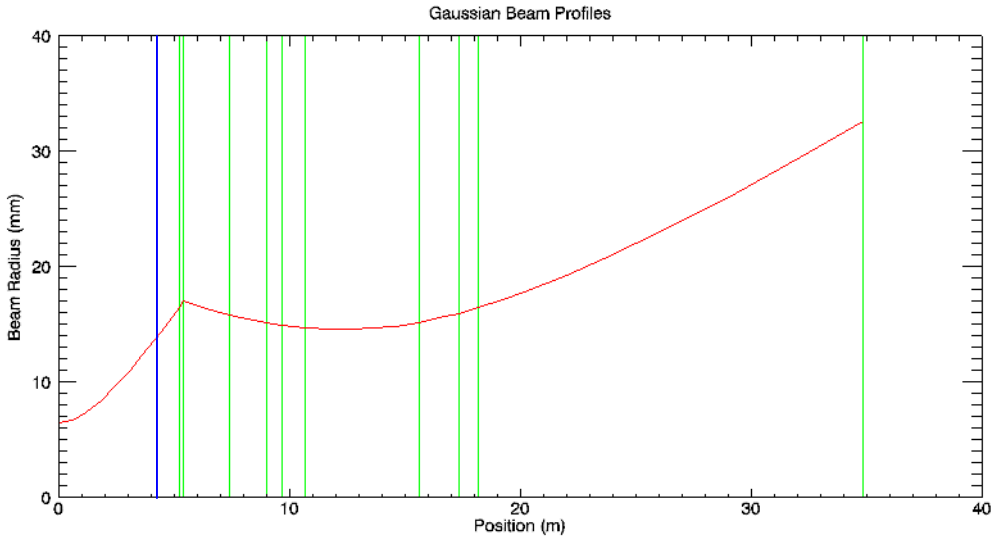

Fig. 5. Same as Fig. 4, but for somewhat different focal lengths (f_{PT408} = 5100 mm, f_{PT417} = 7200 mm).

Using an even longer focal length for PT408 does not have as a result that the beam radius in the access cell (and hence the needed diameter for mirror PT417) becomes smaller. This seems to be in contradiction with our earlier results.[iv] The reason for this apparent discrepancy is that the distance between retro-reflector and second (focussing) mirror is shorter than used in the previous study.

Alignment of the beam and tolerances on optics

The full optical system from PT409 till PT417, and even further to the element closest to laser and/or detector can be made auto-aligning, in a similar fashion as has been done in the FIR interferometer at JT-60U. In this system each mirror is mechanically attached to the transmission lines on either side, in such a way that it always will reflect the beam from the optical axis of one transmission line into that of the other (see Fig. 6), irrespective of any movements of one of the transmission lines. Such a system can be also applied in the ITER polarimeter system. This system of articulated transmission lines will guarantee a proper alignment from laser all the way to first window (PT409).

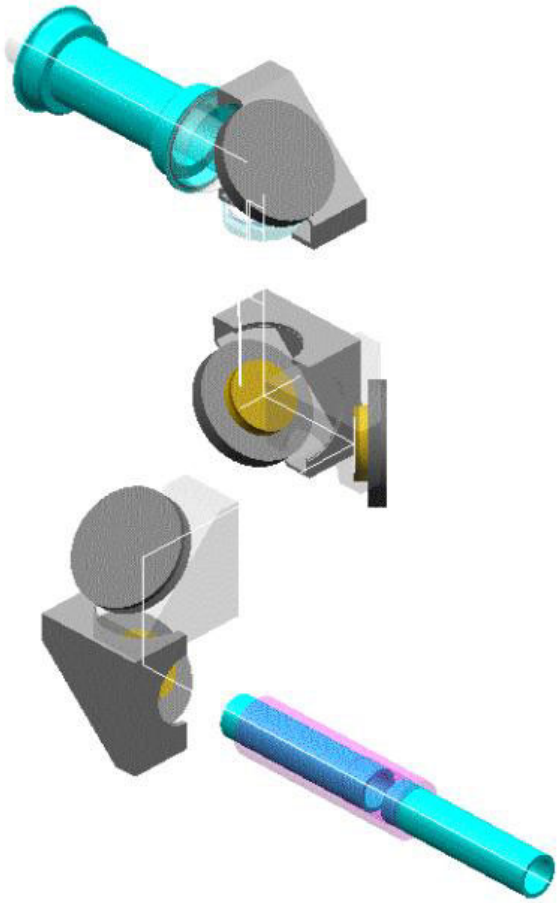

Fig. 6. Articulated transmission lines and mirror assemblies will be used to transport the beam over long distances without any misalignments.

During operation of the polarimeter it can still happen that due to any physical reason (e.g refraction, movement of machine components), the beam is not well aligned onto the retro-reflector, or it may even miss the retro-reflector completely. This can happen for one or more polarimeter chords simultaneously, while other chords maybe still well aligned. The idea is now that as soon as reflection from an individual chord becomes below a certain detection threshold, the chord is automatically scanned from measuring mode to a scanning mode. In the latter mode, the beam is scanned over an area of 100 × 100 mm² at the position of the retro-reflector. Because it is not easy to move the mirrors that are positioned close to the plasma for obvious reasons, it is thought better to do the scanning by tilting one or two mirrors that are further down the beam line. To do the scanning with mirror PT414 seems to be an obvious choice, since this mirror is the first one that is positioned in the access cell. Movement of a mirror in this area will be much simpler than that of a mirror inside the interspace block. Mirror PT414 is positioned at a distance of 15634.64 mm from the retro-reflector. So to displace the beam over ±50 mm at the position of the retro-reflector we need to be able to tilt mirror PT414 over an angle of only ±0.183° or equivalently over ±3.2 mrad, which is easily achievable. This will give an additional displacement of the beam on the optical elements PT407 – PT413, which then defines the totally needed dimension of the beam penetration at each point as well as the needed dimensions of the various optical elements (see Table 3).

Comparing the values in Table 3 with the actual specifications of the transmission lines used in the ITER reference design (see Fig. 7) we must conclude that using a transmission line of 95 mm inner diameter in the interspace volume is not compatible with a scan of the beam over the retro-reflector of ±50 mm in any direction. The inner diameter of the transmission line at the position of PT409 will limit the movement of the beam over the retro-reflector to ±24 mm, which is not enough. In case one takes the 95 mm inner diameter transmission line from PT411 onwards, then the beam scan is limited to ±33.5 mm, which is already much better.

Table 3. Overview of beam diameters at optical components when beam scanning is done by PT414 for f_{PT408} = 4430 mm. Since most mirrors are under an angle of 45° with the beam, the numbers in the right column refer to the direction perpendicular to the plane of the beam. The size of the optical component in the plane of the beam is a factor of √2 larger.

Number	Element	Cumulative distance (mm)	Beam radius (mm)	4.4 times beam radius (mm)	Full displacement for alignment	Required diameter ⊥ beam (mm)
PT406	Retro-reflector	0.00	6.5	28.60	±4.20	37.00
PT407	Plane mirror	5234.10	16.4	72.16	±33.26	138.68
PT408	Spherical mirror	5438.40	17.0	74.80	±32.61	140.02
PT409	First window	7395.73	15.8	69.52	±26.35	122.22
PT411	Plane mirror	9014.00	15.1	66.44	±21.27	108.98
	Second window	9350.00	15.0	66.00	±20.10	106.20
PT412	Plane mirror	9686.00	14.9	65.56	±19.02	103.60
PT413	Plane mirror	10692.00	14.7	64.68	±15.80	96.28
PT414	Plane mirror	15634.64	15.1	66.44	0.00	66.44

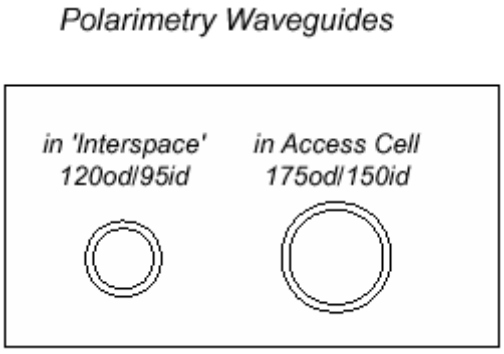

Fig. 7. Specifications of the transmission lines in the interspace block (i.e. from PT409 – PT 414) and in the access cell (i.e. from PT414 – PT417)

Alternatively, one could do the beam scanning with one of the mirrors within the interspace block. Especially when one considers that the full optical set up from diagnostic laboratory to mirror PT411 is made in an auto-aligning fashion, it is purely the beam dimension that determines the required sizes of the optical components. If one uses PT411 for the scanning one needs to tilt the mirror by ±0.32° or ±5.55 mrad to achieve a scan of the beam over an area of 100 × 100 mm² at the position of the retroreflector. The resulting diameters required for the optical component are listed in Table 4. One can conclude that if one scans the beam with a mirror that is mounted in the interspace block (PT411) this will lead to required dimensions of the optical elements in the port plug that are about 20% less then if scanning is done with the first mirror in the access cell (PT414). To first order this will lead to a reduction in the neutron streaming through the port by 36%. However, a drawback will be that the scanning mirror is no longer easily accessible for maintenance and repair. In the next EFDA task it should be investigated which is the better of the two options.

The calculations in Tables 3 and 4 have been done for a focal length of the second mirror of for f_{PT408} = 4430 mm. If one would use the longer focal length of for f_{PT408} = 5100 mm, this would lead to roughly the same conclusions, albeit that the required dimensions of the optical elements in the interspace volume are somewhat larger. The advantage of the longer focal length is that the required diameter of the transmission line at PT417 should by 145.20 mm, which is still smaller than the ITER reference design value of 150 mm.

Table 4. Overview of beam diameters at optical components when beam scanning is done by PT411 for f_{PT408} = 4430 mm. Since most mirrors are under an angle of 45° with the beam, the numbers in the right column refer to the direction perpendicular to the plane of the beam. The size of the optical component in the plane of the beam is a factor of √2 larger.

Number	Element	Cumulative distance (mm)	Beam radius (mm)	4.4 times beam radius (mm)	Full displacement for alignment	Required diameter ⊥ beam (mm)
PT406	Retro-reflector	0.00	6.5	28.60	±4.20	37.00
PT407	Plane mirror	5234.10	16.4	72.16	±20.97	114.10
PT408	Spherical mirror	5438.40	17.0	74.80	±19.83	114.56
PT409	First window	7395.73	15.8	69.52	±8.98	87.48
PT411	Plane mirror	9014.00	15.1	66.44	0.00	66.44
	Second window	9350.00	15.0	66.00	0.00	66.00
PT412	Plane mirror	9686.00	14.9	65.56	0.00	65.56
PT413	Plane mirror	10692.00	14.7	64.68	0.00	64.68
PT414	Plane mirror	15634.64	15.1	66.44	0.00	66.44

Hitherto we mainly discussed the possibility of scanning the beam over the retro-reflector and, in this way, to check the alignment of the system. Furthermore, we have argued in favour of having an articulated transmission line system, that automatically keeps the alignment. Nevertheless, we thought it to be important to also check the sensitivity for misalignments of individual mirrors (angular, transverse and longitudinal misalignment). This was done for mirrors PT414 – PT417, which have all more or less equal sensitivities to misalignment). In Fig. 8 and 9 the power coupling to the retro-reflector are shown as a function of angular and transverse misalignment. The curves for the four mirrors PT414 – PT417 are exactly the same. Therefore only one curve is shown in Figs 8 and 9.

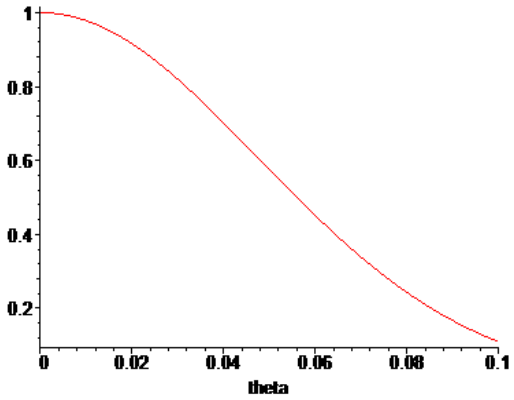

Fig. 8. Power coupling under angular misalignment.

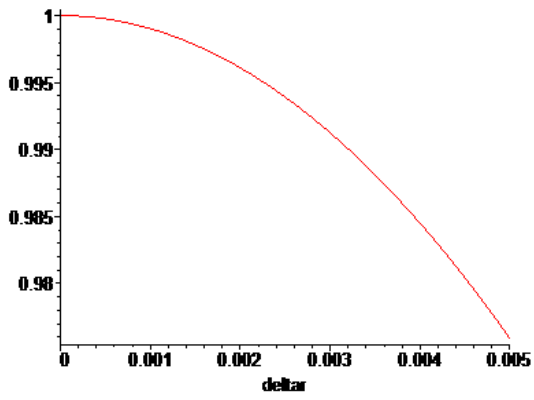

Fig. 9. Power coupling under transverse misalignment (m).

From Fig. 8 one can derive a maximum tolerable angular misalignment of 0.01 rad. The maximum tolerated transverse misalignment is 1 mm in a plane perpendicular to the beam axis. The effect of misalignments along the beam is very low and has not been further considered. These tolerances are not extra-ordinary tough and is must be relatively straightforward to achieve them in a properly designed system.

Calibration

An important sub-task is to develop potential calibration strategies. However, it is very difficult to propose detailed calibration strategies as long as the technical implementation of the polarimeter has not been fixed

(see references [v] and [vi]). Nevertheless, it seems to be a rather obvious way to calibrate the polarimeter between consecutive ITER discharges. In that case, for an ideal optical system the expected Faraday rotation and Cotton-Mouton effect should be zero. However, coatings on especially the first and second mirror, non-ideal behaviour of the retro-reflector, and birefringence in windows can lead to a non-zero rotation of the plane of polarization of the beam as well as to a non-zero ellipticity. The cumulative effect of these can be measured in absence of the plasma.

Future EFDA task should include the study of the various possible technical options for polarimetry (e.g. linear polarization, rocking polarization, rotating polarization). Depending on the choice that will be made, one should look further into the question of calibration to study whether measurements without plasma are sufficient for calibration, or whether additional calibration methodologies should be developed.

Double vacuum boundary

Work has been also done on the design of a double vacuum (and tritium) barrier. This was done in close contact with Chris Walker of the ITER International Team, who accounted for the integration of all designs into the ITER models. The idea is to have two separate windows, both tilted over small angles to avoid disturbances to the signals by reflections. The windows are not placed in the same line of sight, but they are separated by a plane mirror. This has been done to avoid a projectile (i.e. a worst case scenario) coming from the plasma to break both windows. The interspace volume between the two mirrors is separately pumped and monitored (see Fig. 10). The set up as drawn in Fig. 10 has been discussed with and accepted by the ITER safety group.

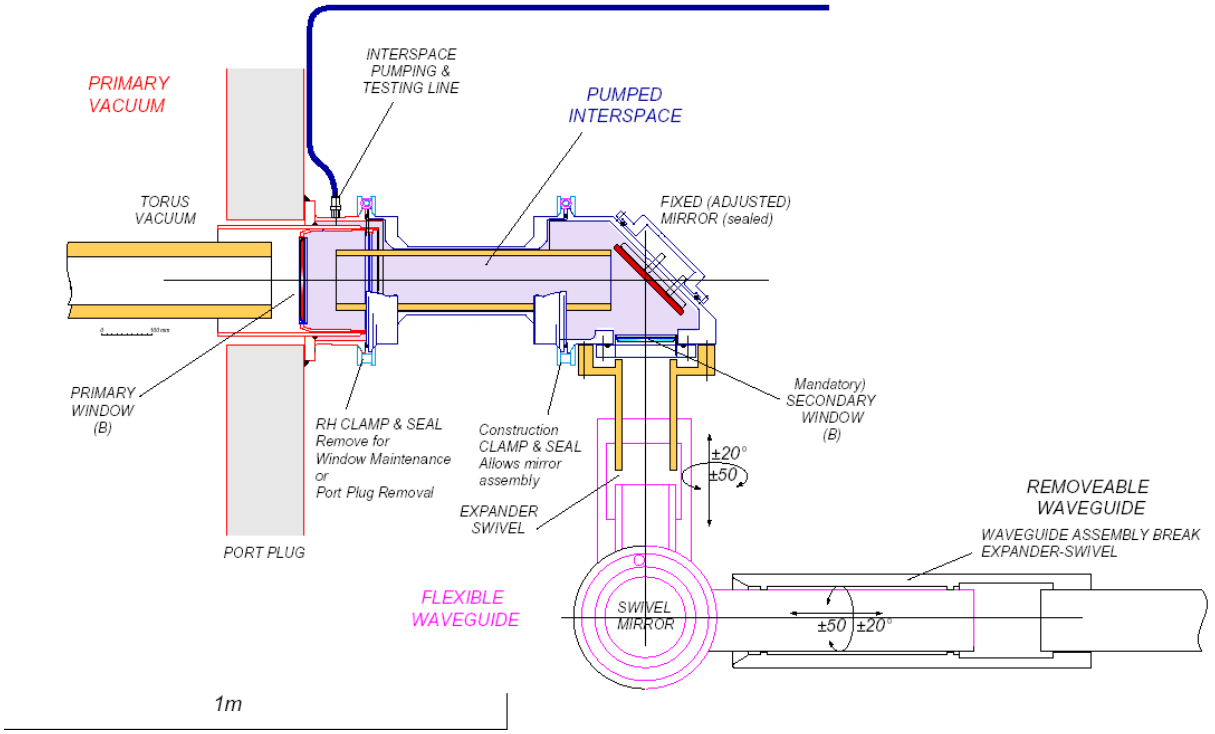

Fig. 10. Design of the double vacuum window. Both the primary and secondary window are mounted under small angles to avoid disturbing effects by reflections. The (shaded) interspace area is separately pumped and tested. Also some details of the flexible transmission line set-up are drawn.

Conclusion

In conclusion one can state that a rather straightforward optical system, featuring two spherical mirrors along with a set of plane mirrors is sufficient to transport the beam from laser to retro-reflector and back. Most of the system can be made self-aligning with articulated transmission lines, but to cope with displacements of the beam at the retro-reflector due to e.g. refractions, movements of machine

components, it is important to have a scanning option. This can be either achieved by a using a mirror inside the interspace block (advantage: smaller mirrors are needed in the port and, hence, smaller neutron streaming through the port; drawback: scanning mirror not easily accessible for maintenance), or by a mirror in the access cell (with opposite advantages and drawbacks). The mirrors should be mounted in the beam line within an angular tolerance of 0.01 rad and a transverse position tolerance of 1 mm.

Two different cases have been studied: one with a focal length of the spherical mirror PT408 of 4430 mm, and one with a focal length of 5100 mm. The first option has the advantage that the dimensions of the optical elements inside the port plug and interspace block are somewhat smaller. However, in the access cell the beam then quickly expands, and in the last 5 meters of the line, the beam does not fit in the reference design transmission lines with 150 mm inner diameter. The second option is fully compatible with the diameter of the transmission lines in the access cell. However, here the dimensions inside the port plug and interspace block are somewhat larger with a disadvantageous effect on the neutron streaming. The forthcoming polarimeter task should address this issue in detail and provide an adequate answer.

A suitable design for the double window has been developed that has been accepted by the ITER safety group.

Acknowledgement

The authors would like to thank George Warr and John Howard of the Australian National University for providing the GRT3D gaussian ray-tracing code. They are furthermore deeply indebted to Chris Walker who converted several of our ideas into conceptual designs.

[ii] A.J.H. Donné *et al.,* 'The poloidal polarimeter system for ITER', in the final report on EFDA Contracts 00-558, 00-559 and 00-560, May 2002.

[ii] G.B. Warr and J. Howard, 'A three-dimensional Gaussian-beam ray-tracing program for designing interferometer/polarimeter plasma diagnostics', Rev. Sci. Instrum. **72** (2001) 2305.

[iii] D. Veron 1979 in *Infrared and Millimeter Waves* (K. J. Button editor), Vol. 2, Academic, New York.

[iv] H. R. Koslowski, 'Calculation of beam diameter, size of port penetrations, and beam line dimensions for the poloidal polarimeter on ITER', in the final report on EFDA Contracts 00-558, 00-559 and 00-560, May 2002.

[v] J.H. Rommers, *et al.,* 'Analysis of phase measurements in combined interferometer and polarimeter systems', Plasma Phys. Control. Fusion 40 (1998) 2073–2080.

[vi] A.J.H. Donné, 'High spatial resolution interferometry and polarimetry in hot plasmas', Rev. Sci. Instrum. 66 (1995) 3407–3423.

Annex II (FOM/Kharkov): Measurements of the reflectance of mirrors composing a corner-cube reflector

MEASUREMENTS OF THE REFLECTANCE OF MIRRORS COMPOSING A CUBE-CORNER REFLECTOR

The final report on Agreement for scientific research collaboration between the Kharkov Institute of Physics and Technology (KIPT) and the FOM-Institute for Plasma Physics "Rijnhuizen" (FOM- Rijnhuizen) from 24 February 2003.

Authors: V.S.Voitsenya, A.F.Bardamid[a], V.N.Bondarenko, V.G.Konovalov, D.I.Naidenkova, I.V.Ryzhkov, A.N.Shapoval, A.F.Shtan', S.I.Solodovchenko, K.I.Yakimov[a]

NSC KIPT, 61108 Kharkov, Ukraine; [a]Taras Shevchenko National University, Kiev, Ukraine

Abstract

The surface roughness of cube-corner reflectors can have a large effect on their reflective properties. In this report the reflective properties of a cube corner reflector are studied at two different wavelengths, 10.6 and 118.8 μm, which are both relevant for interferometry/polarimetry diagnostics envisaged for ITER. The sputtering expected in ITER is simulated by bombardment of the cube-corner reflectors with deuterium ions from a plasma source. Various materials for the reflectors have been studied. One of the conclusions is that if the cube-corner reflectors envisaged for the poloidal polarimeter system in ITER (118.8 μm) are made of polycrystalline molybdenum they will maintain good reflective properties during the full ITER life cycle. This cannot be concluded for the reflectors in the toroidal polarimeter system (10.6 μm), where extensive precautions are required to reduce the sputtering by charge exchange atoms.

1. Introduction

For two plasma diagnostics in ITER the use of cube-corner reflectors (CCR) is envisaged: poloidal and toroidal polarimetry. The multi-channel poloidal polarimetry system is designed to operate at a wavelength of 118.8 [1], and for the multi-channel toroidal polarimetry system a dual CO_2 laser was suggested as a source [2] using simultaneously wavelengths of 10.6 and 9.27 μm.

In spite of the quite long wavelengths to be used in these diagnostics, the long term sputtering by charge exchange atoms (CXA) or the deposition of a carbon-based contaminant layer can affect the properties of the CCR. Therefore, the role of both of these negative factors on the reflective properties of the CCR has to be analysed.

The cube-corner reflectors of the poloidal polarimetry system will be indented not deeply in the blanket construction at the high field side of the ITER device, and therefore the CXA flux will be only slightly weakened in comparison to the flux to the first wall. In addition the mirror surfaces will be bombarded by CXA not along the normal to the surface, which increases the sputtering yield even further. Finally, the back reflected signal passes reflections in series from every CCR mirror with the total reflectance equal to R_0^3 where R_0 is reflectance of a single mirror surface.

For a qualitative evaluation of the effect of the surface roughness on the reflectance, Bennett's formula [3] is frequently used:

$$R = R_0 \exp[-(4\pi d)^2/\lambda^2].$$

Here R is the reflectance of the rough surface, R_0 is the reflectance of an ideal smooth surface, d is the mean surface roughness, and λ is the wavelength of the reflected light. In Fig. 1 the effect of the surface roughness on the reflectance is shown in relative units. As can be seen, at $d/\lambda = 0.02$ the reflectance of the cube-corner reflector has dropped already by ~20% with respect to that of a CCR with smooth surfaces. For $\lambda = 118.8$ μm this happens at $d \cong 2$ μm, but for $\lambda = 10.6$ μm at only $d \cong 0.2$ μm.

The drop of reflectance results in a reduced reflected signal amplitude, which can be overcome to a certain extent by using a stronger laser source or more sensitive detectors. However, as the divergence of the reflected beam can also become worse due to an increased surface roughness, in reality the signal returning back to the receiver can be much smaller. Additionally the increased surface roughness can lead to change of the polarized ellipse of reflecting signal.

2. Motivation of the experimental simulation

To be able to propose suitable materials for the CCR mirrors, it is assumed that the mean surface roughness grows proportionally to the rate of sputtering of the CCR mirror surfaces with a coefficient equal to 0.2, which looks quite reasonable as will be seen from SEM photos below. In such a case our criterion for the permissible loss of reflected signal to be ~20%, means that the total depth of the eroded layer must not exceed 10 μm and 1 μm for the indicated wavelengths, correspondingly. Taking into account the flux and mean energy of CXA to the wall of ITER [4], and the sputtering yields of different metals [5], it is concluded that the depth of the layer eroded by the CXA flux will not exceed 5 μm if molybdenum or ~1 μm if tungsten are chosen as the CCR material. In this estimation it was assumed that the CXA flux to the CCR is attenuated by a factor of three compared to the CXA flux impinging on the first wall, which was calculated [4] to be $\sim 3 \cdot 10^{15}$ at/cm^2·s with a mean atom energy of 200-300 eV. Of the two mentioned candidate CCR materials, molybdenum looks more preferable for technological reasons. For other metals with high reflectance in IR, like stainless steel or copper, the sputtering yield is several times higher than that for molybdenum, and thus they will not satisfy the criterion that the depth of the eroded layer is less than 10 μm during the full ITER life time. (In the estimation of the eroded depth, the effect of ion sputtering was neglected, in spite of the fact that the ion flux to the inner part of the first wall will exceed the CXA flux [4]. This is allowed because the predicted ion temperature [4] is well below the sputtering thresholds for both Mo and W.)

To simulate the effect of long-term sputtering in ITER on the degradation of CCR optical properties, CCR mirror samples have been exposed to deuterium ions from the DSM-2 device [6]. However, to sputter layers of 5 μm depth from three Mo mirrors would take too long a time. Therefore, the main simulation experiments reported in this paper were done with polycrystalline copper mirrors (eroded down to a depth of ~5 μm), because the sputtering rate of copper is about a factor of five higher than that of molybdenum.

Two kinds of copper mirrors were used: polycrystalline oxygen-free copper with a rather small grain size, and a polycrystalline CuCrZr alloy (dispersed-strengthened copper alloy) with a total content of additions (Cr and Zr) not more than 1%. In contrast to oxygen-free copper, where only diamond turned treatment can guarantee a high quality of the mirrors, the dispersed-strengthened copper alloys can be mechanically polished, which significantly

simplifies the process of mirror fabrication. The ion sputtering rates for both materials were found to be very close to each other.

From each kind of material three identical mirror samples were prepared by bombardment with ions from a deuterium plasma until the depth of the eroded layer reached ~5 μm, i.e., similar to the estimated depth of layer that would be eroded due to CXA sputtering of molybdenum CCR mirrors (λ=118.8 μm) in ITER for the total time of reactor operation. SEM photos of surfaces of both mirrors are presented in Figs. 2 and 3.

3. Experiment

First measurements of the reflectance of the dismountable retro-reflector showed that misalignment in the positions of the fixed mirrors (without alignment possibilities) resulted in a significant inaccuracy due to scattering of the reflected beam in such a way that its cross section exceeded the size of the receiving antenna aperture (20 mm). For this reason the retro-reflector was modelled by a system of three separate mirrors as shown in Fig. 4. The beam intensity after reflection from all three mirrors in series was measured.

3.1. Measurements of the reflectivity at λ=118.8 μm

As radiation source a CH_3OH laser was used (λ=118.8 μm) with optical pumping by a CO_2 laser (λ=10.6 μm). The output of the CH_3OH laser radiation was realized through a pupil of 4 mm diameter. A small part of the sub-mm radiation was branched off by a film beam splitter to a pyro-electric detector (P1) and measured by a digital voltmeter (DV1) to control the stability of laser power.

To form the necessary beam waist of the laser beam at the location of the "retro-reflector" (similar to focussing in the ITER poloidal polarimeter [1]), a spherical mirror M1 (R = 1 m) was positioned at 57cm from the laser exit pupil and at a distance of 170 cm a second spherical mirror M2 (R = 2 m). At a distance of 87.5 cm from this second mirror, the beam waist was 6 mm, and exactly at this location the first mirror of the "retro-reflector" was positioned. The entire length of the laser beam from the first mirror of the "retro-reflector" to the pyro-electric detector was $l_1+l_2+l_3 = 9$ cm. The signal from this receiver was measured by a second digital voltmeter (DV2). Then the same pyro-electric detector was placed directly in the laser beam coming from mirror M2, at a position of 9 cm behind the waist, without "retro-reflector", and the signal was registered with the same digital voltmeter (DV2). With such a scheme the absolute reflectance of the "retro-reflector" is determined as the ratio: $R = P_1/P_2 \times 100$ %.

A drawback of the measuring procedure is that there is a probability of an inaccuracy due to the error in the positioning of the detector at every measurement. To decrease the error bar to a value of about ~2%, the measurements were done not less than five times and, moreover, independently by three experimentalists.

The optical system of beam waist formation allowed to have very slow widening of the laser beam: at a distance 7 cm from the beam waist the beam diameter was still only 6.5 mm.

The measurement results are presented in Table 1. The data for single reflection shown in the Table were obtained as the third root of the data measured with three mirrors in series (i.e. the data of the "retro-reflector").

Table 1. Reflectance at λ=118.8 μm of copper mirrors before and after a layer of ~5 μm thickness was eroded due to sputtering by ions of deuterium plasma with a wide energy distribution.

Mirror samples	R before ion bombardment		R after ion bombardment	
	single mirror	"retro-reflector"	single mirror	"retro-reflector"
O-free copper	97.7%	93.5%	97.8%	93.7%
CuCrZr	99.2%	97.6%	97%	91%

It is seen that the reflectance of ion eroded mirror samples fabricated from oxygen-free polycrystalline copper did not change after long-term exposure to bombardment by ions from a deuterium plasma. In contrast, the reflectance of mirrors fabricated from CuCrZr alloy decreased a little. This fact is in qualitative agreement with SEM data for both kinds of mirrors, namely, the surface of the CuCrZr mirrors became rougher than that of the O-free copper mirrors.

The data in Table 1 demonstrate that after a layer of ~5 μm in thickness was eroded, the reflectance of three mirrors at λ=118.8 μm did drop only a little even for polycrystalline copper. If for some reason the rate of CCR sputtering in ITER is 2-3 times higher than was estimated on the grounds of the calculation [4], the use of Mo mirrors still can guarantee that the roughness will stay in a range where the intensity of the reflective signal will have a reasonable value. Even higher CXA fluxes can be tolerated if the CCR's are made from single crystal molybdenum with necessary precaution during the fabrication process (i.e. with minimum mechanical treatment to keep the amount of defects created small). As was shown in simulation experiments, single crystal Mo (and W) mirrors can maintain the reflectance near their initial level even after a 5 μm thick layer was eroded by deuterium ions (e.g. [7]).

3.2. Measurements of the reflectivity at λ=10.6 μm

Approximately the same scheme was used for measurements of the reflectance of the same mirror samples at a wavelength of 10.6 μm. The results are presented in Table 2.

Table 2. Reflectance at λ=10.6 μm of copper mirrors before and after a layer of ~5 μm thickness was eroded due to sputtering by ions of deuterium plasma with wide energy distribution.

Mirror samples	R before ion bombardment		R after ion bombardment	
	single mirror	"retro-reflector"	single mirror	"retro-reflector"
O-free copper	97%	91%	87%	66%
CuCrZr	96%	90%	42%	7.3%
CuCrZr				32%*

*This value was obtained when the scheme of measurement included two non-exposed mirrors and one mirror exposed to bombardment by ions of deuterium plasma. It is less than 42% * 0.96^2 because of the scatter in the reflectance measurements (see Table 3).

It is seen that after sputtering of a ~5 μm thick layer from the mirror, the reflectance of the O-free copper "retro-reflector" is still reasonable at 10.6 μm, but the reflectance of the CuCrZr "retro-reflector" has dropped to an unacceptable low level. However, it is planned to mount the retro-reflectors of the multi-channel toroidal polarimetry system behind the blanket shield modules. They will observe the plasma through quite narrow and long grooves [8]. Therefore, the CXA flux to the CCR's will be strongly attenuated and therefore the CXA sputtering will not play any significant role in the degradation of the optical characteristics of

CCR. In these conditions, the deposition of contaminants (carbon, beryllium) on the CCR surface can become the main factor of degradation.

Hitherto, the effects of such contaminants on the optical characteristics of mirrors were analysed only in the visible spectral range [9]. This work needs to be extended to the 10 μm wavelength range to understand the potential degradation of the reflective properties of the CCR's used in the toroidal polarimeter system.

The scheme shown in Fig. 4 was also used for investigating the effect of the surface roughness on the polarization angle of the reflected beam at λ=10.6 μm. The details of these particular measurements are given in Fig. 5 and the results are presented in Table 3. In the insert of Fig. 5 the polarization of the initial probing beam is indicated: the electric field is parallel to the surface of the mirror M1 for the case Phor. The measurements #1-#3 were provided for the following combinations: two non-exposed Cu mirrors and one CuCrZr mirror eroded down to ~5 μm; in the scheme #4 all three mirrors were eroded; in the scheme #5 only non-exposed mirrors were used. From the results obtained we can conclude that the roughened surface causes a significant change of both the reflectance and polarization angle of the reflecting beam. The effects strongly depend on the initial polarization of the probing beam and are maximal for the horizontal orientation of the electric field, i.e., when the electric field is parallel to the surface of mirror M1. In a real retro-reflector scheme the same situation cannot be realized. Instead, the effects for a real CCR will be between those shown for "vert" and "hor". It should be noted that the data of Table 3 demonstrate that in spite of the initial similarity of all mirrors, the eroded samples have different characteristics both for the reflectance and for polarization angle change.

Table 3. Reflectance and polarization angle change measured by the scheme shown in Fig.4 and 5 for three initial polarizations of the probing beam (λ=10.6 μm).

##	Combination of mirrors	Reflectance for indicated polarization			Angle of rotation of the polarizer to obtain the maximal signal		
		R_{vert}	R_{hor}	$R_{45°}$	φ_{vert}	φ_{hor}	$\varphi_{45°}$
1	$M_1(I_1)$; $M_2(I_2)$; $M_3(E_1)$	52%	29%	41%	~0	1°	~0
2	$M_1(I_1)$; $M_2(I_2)$; $M_3(E_2)$	48%	22%	35%	~0	2.8°	~0
3	$M_1(I_1)$; $M_2(I_2)$; $M_3(E_3)$	50%	23%	36%	~0	3.1°	~0
4	$M_1(E_1)$; $M_2(E_2)$; $M_3(E_3)$	12%	2%	7%	~0	8.9°	~0
5	$M_1(I_1)$; $M_2(I_2)$; $M_3(I_3)$	95%	92%	93%	~0	~0.5°	~0

Symbols I_1, I_2, I_3 are for non-exposed mirrors, and symbols E_1, E_2, E_3 are for mirrors eroded by ion sputtering down to the depth ~5μm.

Also experiments with Mo mirrors were performed. This was not done for CCR's but for single mirrors. The behaviour of a high-quality Mo (111) mirror was compared to that of an imperfect Mo (100) mirror by measuring the reflectance in the wavelength range λ = 253 - 600 nm, where the effect of reflectance degradation could be measured with confidence. The high-quality (111) mirror sample was prepared with minimal mechanical treatment, namely, the cutting procedures were done by means of spark cutting and the polishing procedure was very laborious, with gradual decrease of the size of powder up to the last size only ~100 nm.

This process was started with ~3 μm size of diamond powder particles; then moved to ~1 μm and the layer with thickness not less than 3 μm was removed; next powder ~300 or ~500 nm in size and again polished to the depth not less than previous powder size, i.e., 1 μm, etc. With ~100 nm powder particle size the eroded layer was approximately equal in depth to the next to last size of powder particles. The Mo(100) mirror was produced without these precautions.

The data on the absolute reflectance for two wavelengths as a function on the depth of layer eroded due to ion sputtering are shown in Fig. 6. A strong decrease in the UV and visible part of the spectrum has been observed for the (100) Mo sample, but no measurable decrease of reflectance was observed at λ=118.8 μm. The reflectivity of the Mo (111) mirror is rather insensitive to the thickness of the eroded layer, even at 118 μm. These results are presented here because the rate of degradation of the (100) Mo mirror looked quite close to the degradation of a polycrystalline Mo mirror, thus – rather similar to the rate of degradation of polycrystalline Cu mirrors studied in this investigation, but not shown in Fig. 6. It is concluded from our experimental results with different Mo samples that if one doesn't follow the careful and laborious manufacturing process described in the previous paragraph, the monocrystalline material looses much of its advantage in robustness against long-term sputtering. Because the construction of the retro-reflector is quite complicated, it is probably difficult to apply the elaborate polishing procedure and this, in turn, leads to a high level of structural defects in the near surface volume and in the bulk. Therefore, it is thought that there is not a substantial advantage of a single crystalline CCR above a polycrystalline CCR.

If however, methods are developed to manufacture a single crystalline CCR with similar precautions as for the (111) Mo mirrors described above, the CCR would be more resistant to the development of the micro-relief than the one fabricated from polycrystalline material. Nevertheless, one may wonder whether this is really needed, since it was clearly demonstrated in this report that CCR's made of polycrystalline molybdenum are already expected to function properly during the full ITER life time.

One additional note concerns the effect of the structure of the mirror material on the rate of mirror degradation. It was found in the course of the simulation experiment that a Cu mirror with a large grain size (up to ~1 mm) has a higher resistance to long-term bombardment by deuterium plasma ions than the Cu mirror with a small grain size (of the order ≤ 0.1 mm). The reason of this important fact is not understood yet.

4. Conclusions

1. It was assumed that sputtering by CXA will be the main reason of degradation of the reflectivity of Mo retro-reflectors used in the poloidal polarimeter. It was estimated that a layer of ≤ 5μm thickness will be eroded from the mirror surfaces for the whole operational life time of ITER.

2. In simulation experiments the effect of long-term sputtering up to a depth of ~5μm by deuterium ions from a plasma with a wide energy distribution on the reflectance at λ = 118.8 μm and λ = 10.8 μm was measured for two kinds of polycrystalline copper mirror samples: 1) oxygen-free copper samples with a small grain size were prepared by diamond turning; 2) samples from a CuCrZr alloy (dispersed-strengthened copper alloy) were prepared by mechanical polishing.

3. The results obtained in experiments with Cu mirror samples show that sputtering of the top 5 μm layer from a polycrystalline Mo mirror would not result in a noticeable decrease of reflectance at λ = 118.8μm, and thus polycrystalline molybdenum can be recommended as material for fabrication of retro-reflectors for this specific plasma diagnostic.

4. For the toroidal polarimetry system operating at much shorter wavelengths (λ=10.8μm) a similar rate of sputtering is absolutely inadmissible. This is also because the path length of the probing beam is much longer than that of the poloidal polarimetry system. Therefore, the divergence of the reflected beam would play a more serious role. To avoid this, the geometry of the holes in (or behind) which the Mo retro-reflectors are mounted, have to provide an attenuation of the CXA flux to the CCR surface by more than an order of magnitude as compared to that at the first wall flux.

5. It was found that under bombardment by deuterium ions from a plasma, the optical properties of an imperfect single crystalline Mo mirror degrade almost as fast as the optical properties of polycrystalline mirror. It follows from this fact that due to the high degree of mechanical treatment needed for fabrication of retro-reflectors, the CCR samples fabricated from single crystalline material would loose those advantages.
However, as can be concluded from results presented above, for sub-mm methods of diagnostics CCR fabricated of polycrystalline molybdenum are expected to have reasonable reflective properties during the full ITER life time.

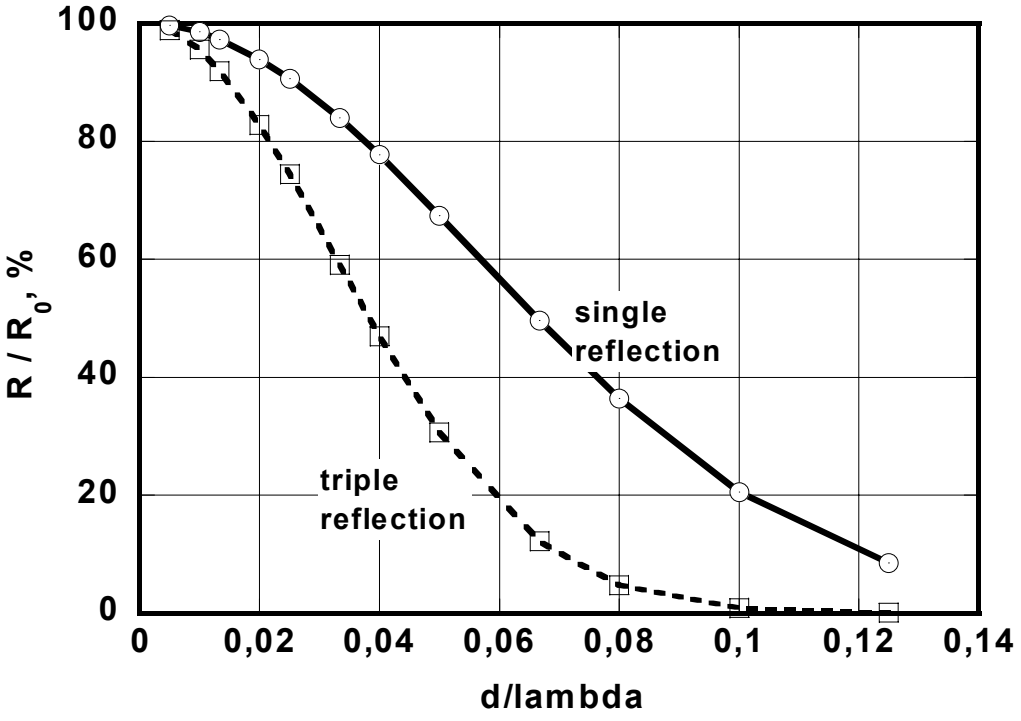

Fig. 1. The reflectance of a metal mirror as a function the mean roughness according to Bennett formula.

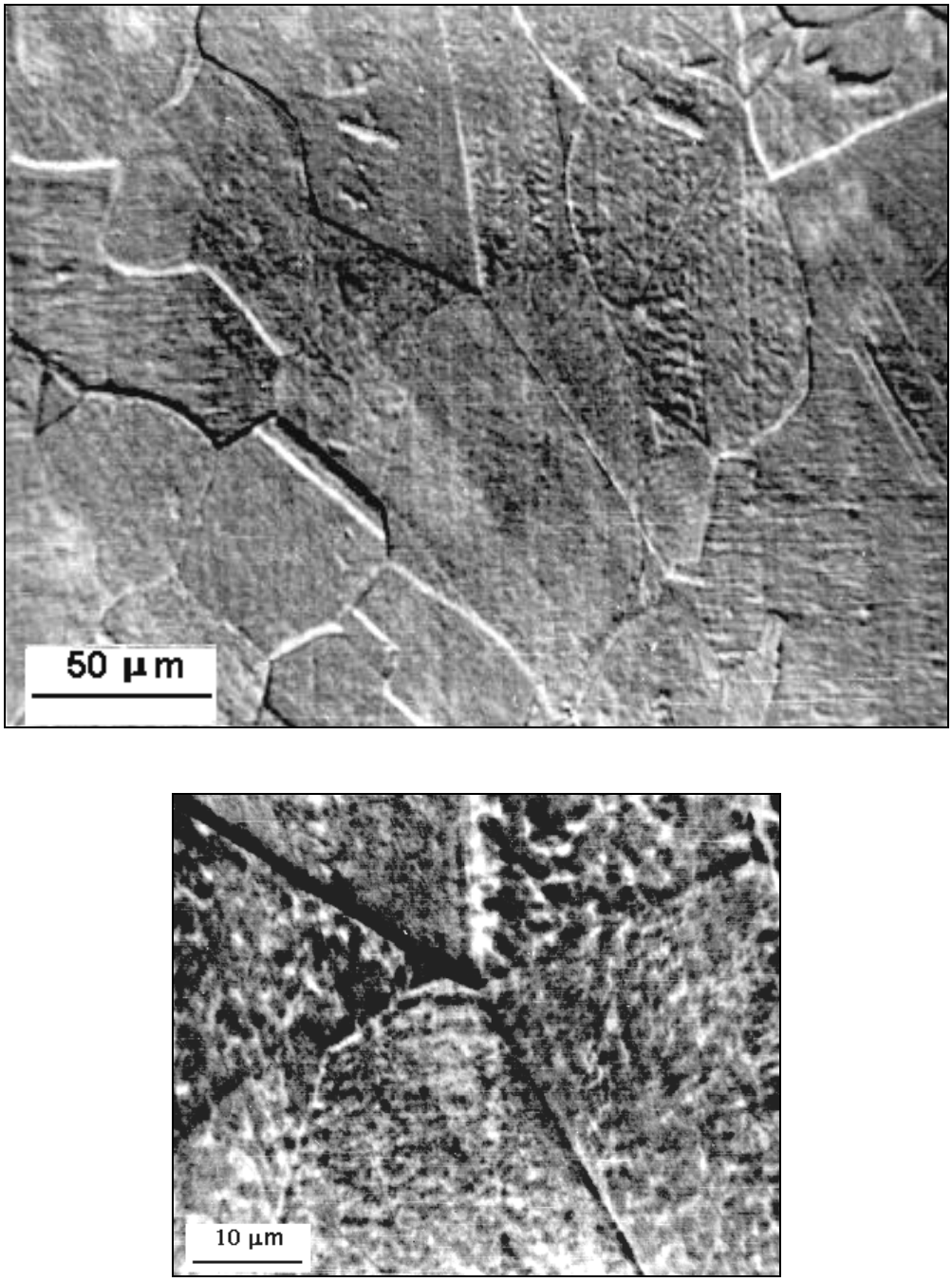

Fig. 2. SEM photos with different magnifications of the surface of a mirror fabricated from oxygen-free copper after layer of ~5 µm thick was eroded by ion sputtering.

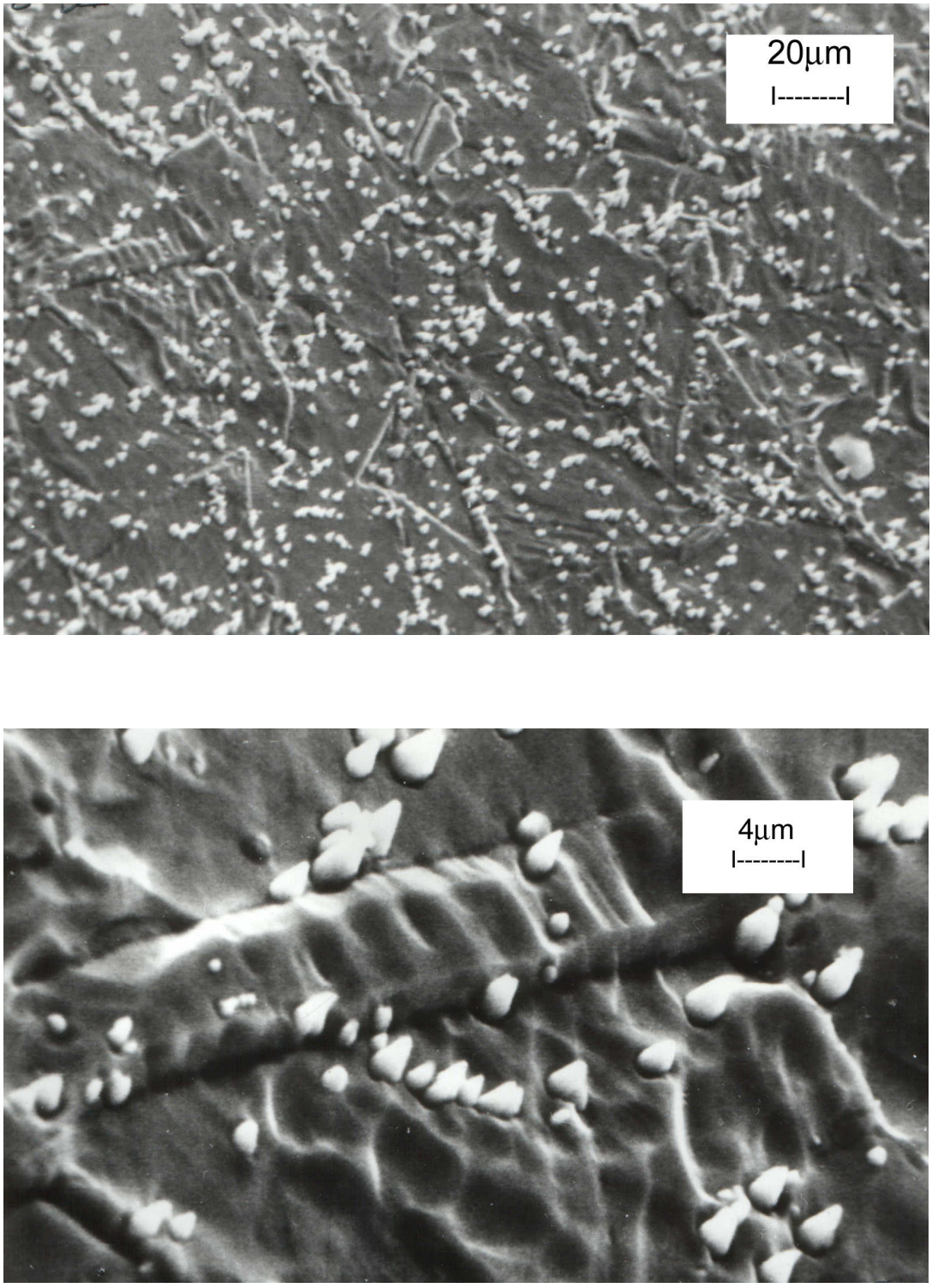

Fig. 3. SEM photos of the surface of the CuCrZr mirror after a layer of ~5 µm was eroded by ion sputtering. The cone-shaped artefacts on the surface are precipitates of dopans (Cr, Zr) in the bulk of the alloy. They became visible due to their lower rate of sputtering compared to that of the Cu matrices.

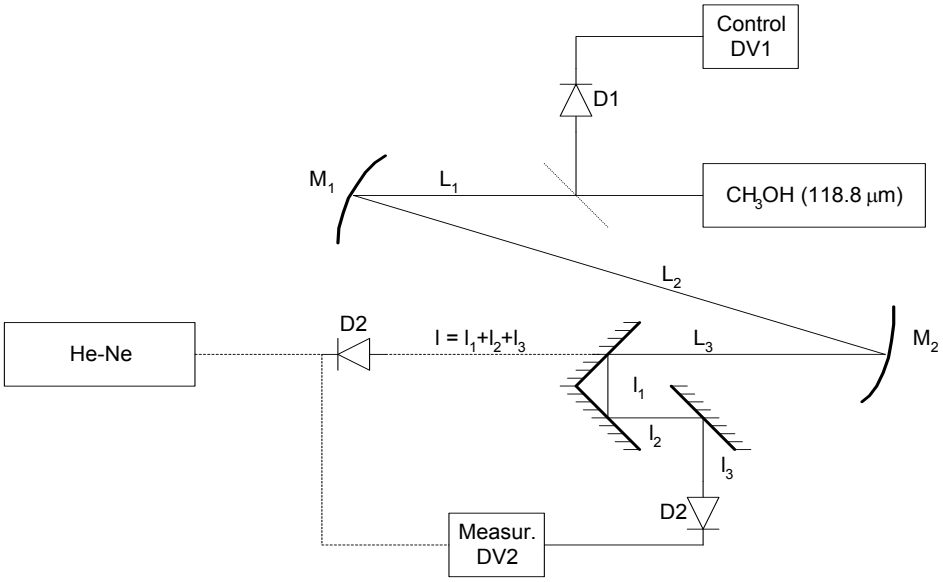

Fig. 4. Scheme to measure the total reflectance of three mirrors in series at the wavelength 118.8 μm. The description of scheme is in the text. The oxygen-free Cu mirrors have a size of 22x22x4 mm^3, the mirrors of CuCrZr alloy are circular with a diameter 22 mm and thickness of 4 mm.

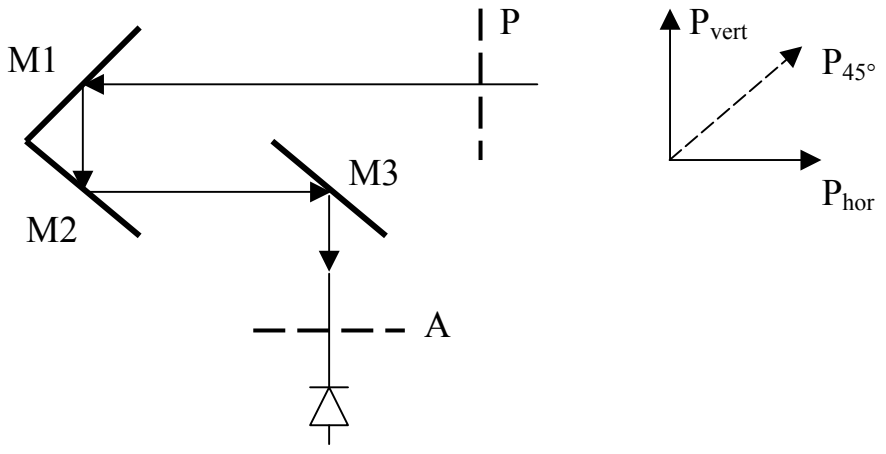

Fig. 5. The scheme of measurements of surface roughness effect on the change of polarization angle.

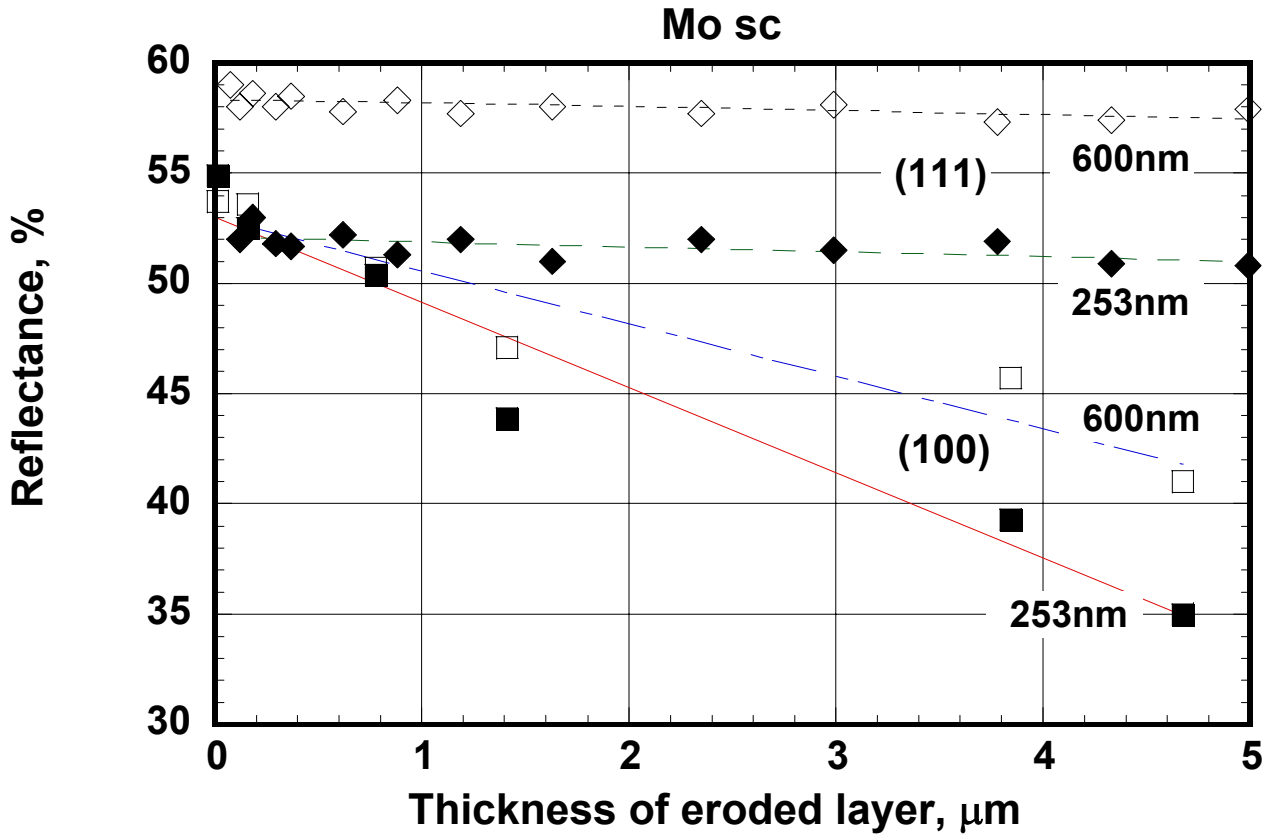

Fig. 6. Comparison of reflectance at indicated wavelengths of plane mirrors fabricated from high-quality (111) (diamonds) and imperfect (100) (squares) Mo single crystals depending on the depth of layer eroded due to bombardment by ions of deuterium plasma with wide energy distribution.

References

1. A.J.H. Donné, M. Cavinato, C. Gil *et al,*. A poloidal polarimeter system for current density measurements in ITER. Proc. 11th Int. Symp. on Laser-Aided Plasma Diagnostics, Les Houches (2004) paper S1.
2. Y. Kawano, Sh. Chiba, A. Inoue, Infrared polrimetry for electron density measurement in tokamak plasmas, Rev. Sci. Instrum. **72** (2001) 1068.
3. H.E. Bennett. JOSA, **53,** 1389 (1963).
4. R. Behrisch, G.Federici, A.Kukushkin, D.Reiter, Material erosion at the vessel walls of future fusion devices, J. Nucl. Mater. **313-316** (2003) 388.
5. Y. Yamamira, H. Tawara, Energy dependence of ion-induced sputtering yields from monoatomic solids at normal incidence, ADNDT **62** (1996) 149.
6. A.F. Bardamid, V.T. Gritsyna, V.G. Konovalov, *et al,* Ion energy distribution effects on degradation of optical properties of ion-bombarded copper mirrors, Surf. Coat. Technol. **103-104** (1998) 365.
7. A.J.H. Donné and A.E. Costley for the ITPA TG on Diagnostics. Key Issues in Diagnostics for Burning Plasma Experiments, IEEE Transact. on Plasma Sci. **32** (2004) 177.
8. T. Kondoh, Y. Kawano, A.E. Costley, *et al*., Toroidal interferometer/polarimeter density measurement system for long pulse operation on ITER, in Proc. of 30th EPS Conference on Controlled Fusion and Plasma Physics, St-Petersburg, (2003), Paper P-4.64.
9. A. Malaquias, M. von Hellermann, P. Lotte, *et al.*, Polarization and reflectivity changes on mirror based viewing systems during long pulse operation, in Proc. of 30th EPS Conference on Controlled Fusion and Plasma Physics, St-Petersburg (2003), Paper O-3.4C.

Annex III (ENEA-RFX): Experimental test of a single-chord ITER-like polarimeter configuration

Final Report of EFDA Contract 02-1000
polarimeter task

L. Giudicotti[1], C. Nyhan[1,2] S. L. Prunty[2]

1) Consorzio RFX, Associazione EURATOM-ENEA sulla Fusione
Corso Stati Uniti 4, 35127 Padova, Italy

2) Department of Electrical and Electronic Engineering,
Association EURATOM-DCU, University College Cork, Ireland

Introduction

The purpose of the contract was to perform a test of a single chord FIR polarimeter in a configuration similar to that proposed for ITER and identify factors influencing the measurement. The key requirements for simulating the conditions of ITER, deduced from previous studies[1,2] are: 1) a FIR laser source at $\lambda = 118.8$ μm; 2) modulation of the polarization state of the probing beam; 3) a propagation path of several tens of meters; 4) inclusion of a metallic corner-cube retroreflector in the polarimeter path; 5) simultaneous measurement of the Faraday rotation and of the Cotton-Mouton effect; 6) a resolution equal or better than 1° for changes in the azimuth and ellipticity angles associated to the Faraday and Cotton-Mouton effects; 7) a time resolution equal or better than 10 ms.
The study has been carried out by performing two different experiments. In the first experiment, performed at the Consorzio RFX in Padova, Italy, the FIR laser system and the FIR beamline of the polarimeter of the RFX Reversed Field Pinch machine has been used to reproduce as much as possible the layout of the ITER polarimeter; a parallel experiment with a simpler layout was carried out at the Department of Electrical and Electronic Engineering of University College Cork, Ireland, to demonstrate a better time resolution of the same polarimeter method.

The experiment at Consorzio RFX.

The conceptual layout of the single chord polarimeter experiment initially planned at the RFX laboratory to simulate as much as possible the ITER conditions is shown in Fig. 1.

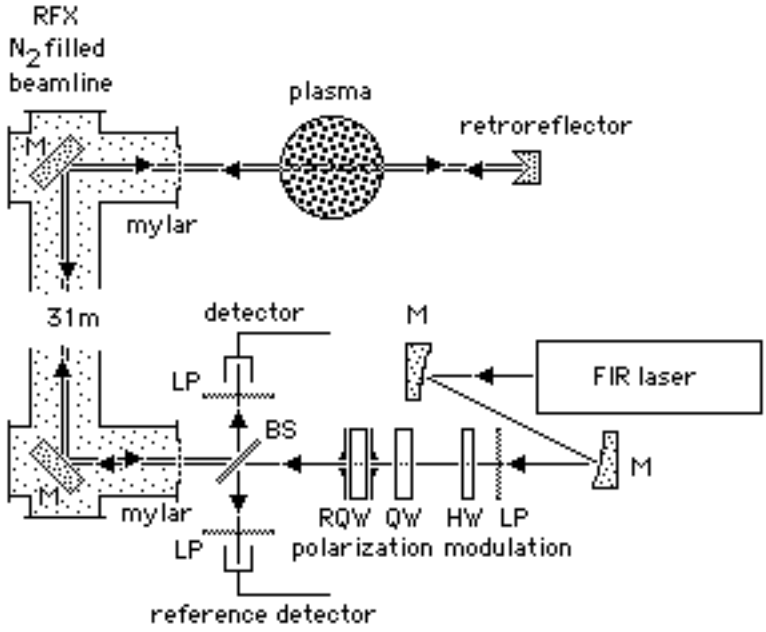

Fig 1 - Conceptual layout of the single-chord, retroreflected polarimeter experiment planned at RFX. M: mirror, LP: linear polarizer, HW: halfwave plate, QW: quartewave plate, RQW: rotating quarterwave plate.

Eventually measurements with this set-up were unsuccessful. The study however was satisfactory completed by successfully performing a series of experiments in a very similar arrangement.

The experimental apparatus

1) The FIR laser

The radiation source is a CO_2 pumped, FIR laser from Edinburgh Instruments. The CO_2 laser (model PL6) can provide pump power in excess of 100 W CW. The FIR cavity is of the dielectric waveguide type (model 295) and uses CH_3OH as the laser medium. The maximum FIR output power is ~ 300 mW CW at λ=118.8 μm and the output radiation is linearly polarized in an horizontal plane. We assume this direction to be the direction of the reference *x*-axis, so that the FIR output beam will be in a linearly horizontal polarization state (LHP). For operation in the RFX polarimeter the output FIR beam is intensity modulated to a 3 kHz square-wave, by a mechanical chopper on the pump CO_2 beam. The present measurements however required polarization modulation rather than intensity modulation. Therefore the mechanical chopper was removed and a CW FIR output was used, the polarization

modulation being provided by the modulator described below. The two mirrors at the output of the FIR laser constitute a telescope whose purpose is to adapt the FIR beam to the optics of the 31 m-long FIR beamline. After the telescope a linear polarizer restores the LHP polarization.

2) The modulator

The polarization modulator consists of a half-wave plate mounted on a manual rotation stage whose purpose is to control the direction of the linear polarization of the FIR beam, then a fixed quarter-wave plate set at 45° to the reference direction and second quarterwave plate mounted on a rotation stage rotated at a frequency of 20 Hz by a DC electric motor. This set-up generates a polarization modulation scheme proposed by Segre [3,4] in which the azimuth and the ellipticity of the FIR beam change in time at twice and four times the rotation frequency respectively. This polarimetric technique was named by Segre "the U-Method."

3) The FIR beamline

After the polarization modulator the beam is sent into the FIR beamline of the RFX polarimeter. The FIR radiation would be remarkably absorbed by the water vapour if propagated in ambient air. The purpose of the beamline is to provide a medium free of water vapour where the FIR beam can be propagated with virtually no absorption from the RFX FIR laser cabin to the machine vacuum vessel[5,6]. The beamline comprises a set of 10 mirrors mounted inside three air-tight boxes, connected to each other by plastic pipes. All mirrors are spherical, and are made of glass with the reflecting surface covered by aluminum and have a diameter between 100 and 200 mm. The last mirror is parabolic. One of the spherical mirrors deflects the FIR beam by 120° and the last parabolic mirror deflect the beam by 90°. All the other mirrors operate at about normal incidence. The entrance and exit windows are two mylar sheets. The last parabolic mirror focuses the FIR beam to a spot with a waist of 7.6 mm diameter (at $1/e$ of the central intensity), located at a distance of 2.5 m from the beamline output window. During RFX operations, this distance corresponds to the center of the plasma. In this experiment however the RFX vacuum vessel is not in its position and the focus is in air. The entire beamline is filled by a continuous flow of N_2, kept at 30 mbar of overpressure, by a controlled leak (3 li/hr). The mirror diameter and the dimensions of the plastic pipes are considerably larger than the beam diameter so that the propagation in the beamline is essentially a free-space propagation. The entire beampath traversed by the FIR beam is 31 m. The distance traversed by the beam and the number of mirrors are very similar to those expected in ITER so that the RFX beamline can conveniently simulate the ITER polarimeter conditions. However, in the RFX polarimeter the polarization of the input beam is fixed and the plasma is probed in a single passage.

Therefore no particular care was taken to design the beamline for propagation of a polarization modulated beam and for its use in a double pass polarimeter configuration.

4) The retroreflector and the plasma simulator

The FIR beam is backreflected into the beamline by a corner-cube retroreflector located at the waist of the focused beam. This element was provided by the polarimeter team of CEA-Cadarache and is identical to those already in use in Tore Supra [7]. The retroreflector is made of a copper alloy and has an useful area of 50 mm diameter that easily accommodates the 7.6 mm diameter of the focused FIR beam. The characteristics of the retroreflector as well as the results of reflectivity testing are available[8].
The change of the polarization state introduced by the plasma has been simulated by using a half-wave plate and a quarter-wave plate with the axis aligned each other and set at 45˚ with respect to the reference direction. Theory shows that small rotations of this element around this position can conveniently simulate both the Faraday rotation and the Cotton-Mouton effect introduced by the plasma [9]. However for reasons discussed later the plasma simulator was not located in the position indicated in Fig. 1, but at the end of the polarimeter path, in front of the analyzer.

5) The analyzer and the detectors

The return beam at the end of the beamline is separated from the forward beam by the beamsplitter and sent to an analyzer consisting of a linear polarizer set at 45˚ followed by a room temperature pyroelectric detector. This is one of the detectors used for the RFX polarimeter [5,6]. A second identical polarizer/detector assembly is used to provide a reference signal by detecting the forward beam reflected from the beamsplitter.

Selection of the beamsplitter

The first experimental step was the selection of a suitable beamsplitter (BS). This element is very critical in the polarimeter set-up described. Ideally the beamsplitter would have a 50/50 power splitting ratio and conserve the polarization state for both the transmitted and reflected beams. Theoretical values for the transmission and reflection coefficients of various possible materials, have been calculated by C. Gil for incidence angles of 7˚ and 60˚ [see appendix]. For this study we have experimentally tested two different beamsplitters for an incidence angle of 45˚: a) a kapton film, 25 μm thick [10,11]; and b) a square metal mesh [12,13]. For this experimental test, fixed states of polarization have been produced by setting the

modulator elements at fixed angular positions. Tables 1 and 2 show the measured power of the reflected and transmitted radiation for some polarization states of the incident radiation.

25 μm Kapton film @ 45˚	
LHP	LVP
T = 84.1 %	T = 64.2 %
R = 4.4 %	R = 26.32 %

Table 1 - Transmitted and reflected power (as a percent of the incident power) for the kapton BS, for two different polarization states of the incident radiation. LHP: linear horizontal polarization; LVP: linear vertical polarization. The incidence angle on the beamsplitter is 45˚, the transmitted and reflected beam are in the horizontal plane.

metal wire mesh @ 45˚		
LHP	LVP	L45P
T = 36.76 %	T = 33.66 %	T = 36.40 %
R = 39.22 %	R = 41.58 %	R = 41.40 %

Table 2 - Transmitted and reflected power (as a percent of the incident power) for the metal wire mesh beamsplitter. L45P: linear polarization at 45˚.

The kapton film showed transmission and reflection coefficients not very different from the theoretical values, but has a splitting ratio which is significantly polarization dependent and therefore it is unsuitable for use as a beamsplitter in our experiment. The metal mesh has a power splitting ratio approximating 50/50, which is weakly dependent on the input polarization state and thus it is suitable for our requirements. In all the following measurements the kapton film has been used as a ~ 10/90 BS on the LHP beam at the laser output to monitor the FIR output power fluctuations.

A preliminary test on the polarization state of the emerging radiation indicates that the BS introduces some ellipticity both in the reflected and transmitted beams. Therefore we have tried to characterize its polarization properties by measuring its Jones matrix. For this we used the well known method in which the power transmitted past a linear polarizer is measured for three different orientations of the polarizer axis [14]. The measured Jones matrices (normalized) for the transmitted and reflected radiation are:

$$\boldsymbol{J}_{\mathrm{T}} = \begin{bmatrix} 1 & 0.26\,i \\ 0.25 & 0.95 \end{bmatrix} \qquad \boldsymbol{J}_{\mathrm{R}} = \begin{bmatrix} 1 & 0.198\,i \\ 0.289 & 0.95 \end{bmatrix}$$

these matrices should be compared with the Jones matrix of an ideal beamsplitter:

$$\boldsymbol{J}_{\mathrm{BS}} = \begin{bmatrix} 1 & 0 \\ 0 & 1 \end{bmatrix}$$

The measurements confirm that some amount of ellipticity is introduced by the BS. These results are consistent with earlier measurements on copper meshes [13].

As an alternative approach we have also characterized the metal mesh beamsplitter from the point of view of the Mueller calculus, by measuring its Mueller matrices. For this measurement we have used the method of the Fourier analysis of the signal obtained by a rotating quarter-wave plate and a linear polarizer [15,16]. This technique is usually employed for measuring the four components of the Stokes vector of unknown radiation. However if the polarization state of the radiation incident on the beamsplitter is known, then it can be used to obtain four elements of its Mueller matrix.

For this measurement again fixed states of polarization have been produced by setting the modulator elements in fixed positions, and we have assumed that the beamsplitter behaves as an attenuating retarder so that it can be represented by a simplified Mueller matrix of the ABCD type [15]. The above Fourier technique has been implemented by measuring a single period of the waveform obtained by the rotation of a quarterwave plate mounted on a PC controlled, step-motor rotation stage. Two thermal radiometers have been used, one for measuring the signal and one for monitoring the FIR laser power fluctuations. The two radiometer outputs have been digitized by a two-channel digital multimeter and have been digitally processed to equalize the measurement bandwidths. The ideal and the measured (ABCD) Mueller matrices obtained are:

$$\boldsymbol{M}_{\mathrm{BS}} = \begin{vmatrix} 1 & 0 & 0 & 0 \\ 0 & 1 & 0 & 0 \\ 0 & 0 & 1 & 0 \\ 0 & 0 & 0 & 1 \end{vmatrix} \quad \boldsymbol{M}_{\mathrm{T}} = \begin{vmatrix} 1 & 0 & 0 & 0 \\ 0 & 1 & 0 & 0 \\ 0 & 0 & 0.95 & -0.03 \\ 0 & 0 & 0.03 & 0.95 \end{vmatrix} \quad \boldsymbol{M}_{\mathrm{R}} = \begin{vmatrix} 1 & -0.3 & 0 & 0 \\ -0.3 & 1 & 0 & 0 \\ 0 & 0 & -0.95 & 0.01 \\ 0 & 0 & -0.01 & -0.95 \end{vmatrix}$$

These results are consistent with the measured Jones matrices. The degree of polarization (not included in the Jones matrix representation) of the transmitted and reflected radiation was found to be about 0.9, indicating that the BS may introduces also some depolarization. However this measurement method was found to give considerable errors for measuring specific states of polarization. In addition occasionally non physical Stokes vectors, i.e. with polarization index higher than unity were obtained. Therefore these results need to be confirmed by better measurements in the future.

Recommissioning of the RFX FIR beamline.

The next step was the recommissioning of the RFX FIR beamline, which has not used (and was partially removed) after the RFX laboratory fire at the end of 1999. The beamline components have been reassembled and the operation of the N_2 filling system has been resumed. After the matching telescope at the beamline input was reassembled and the FIR beam carefully realigned, a transmission of about 50% was measured with an excess pressure of 20 mbar of N_2. The beam profile at the beamline output was also measured with a pyroelectric array detector to confirm proper focalization. Then the polarization characteristics of the beamline have been checked. Fig. 2 shows the measured data and the fitted function that represents the angular dependence of the measured signal for a LHP beam at the input. Fig 3 shows the polarization ellipse (reconstructed from the measured Stokes vector components)

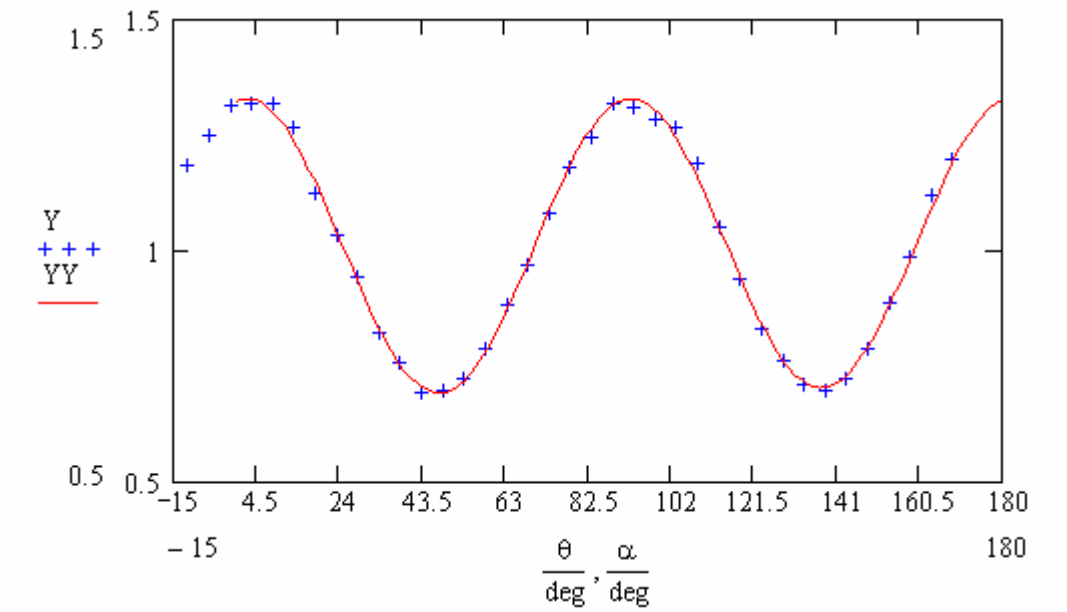

Fig. 2 - Example of data measured by the rotating quarter-wave method. The data points represent the measured power through a linear polarizer as a function of the orientation.
of the axis of the rotating QW plate and the curve is the signal reconstruction .

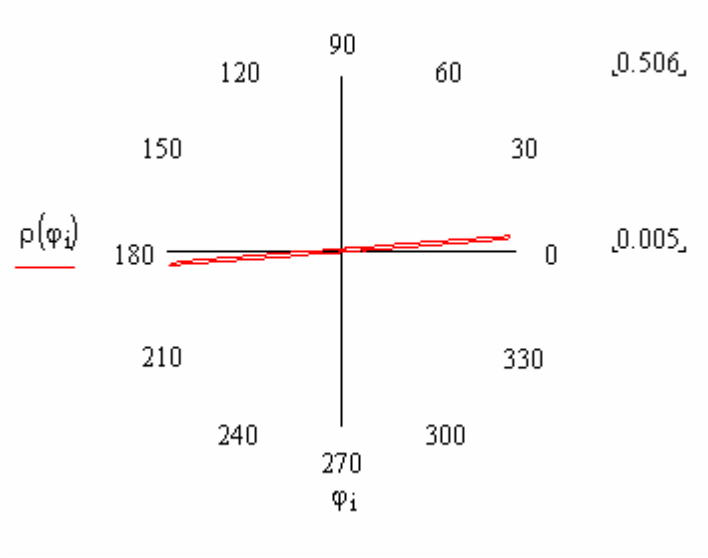

Fig. 3 - The polarization ellipse of the radiation transmitted by the RFX beamline, deduced from data of Fig. 2. The ellipse has azimuth $\psi = 4.5^\circ$ and ellipticity angle $\chi = -0.3^\circ$. The degree of polarization is P = 0.90.

The small value of the azimuth is probably due to a lack of parallelism between the input and output reference planes and can be neglected. For practical reasons the 0° direction in Fig. 3 actually refers to the laboratory vertical direction. In fact the beamline introduces a 90° rotation of the polarization plane as a result of the spatial orientation of the mirror chain. The small ellipticity angle is within the experimental error so that we can assume that 90% of the LHP input radiation is converted to LVP radiation and 10% to unpolarized radiation by the beamline. These results have been confirmed also by a polarization analysis based on the Jones calculus. Here the important result is that beamline has an approximately ideal behaviour, with a low depolarization ratio. In fact, given the structure of the plasma Mueller matrix (also known as the transition matrix), it can be show that no information can be extracted from unpolarized radiation and therefore the FIR power of the unpolarized part of the transmitted beam is lost for diagnostic purposes. On the other hand, a fixed modification of the polarization status of the FIR beam by the beamline can be measured in advance and taken into account in the data analysis so that it does not prevent the operation of the polarimeter. In conclusion the results of this preliminary test indicated that the beamline should be compatible with the operations of a polarimeter in the conditions of ITER, although a complete and conclusive test should be made with a polarization modulated beam. Therefore no further test have been made on the beamline with fixed polarization states.

The polarimetric method.

The polarimetric method chosen for this experiment is the "U-Method" proposed by Segre [5,6]. This technique is based on the polarization modulation scheme provided by the rotating quarter-wave modulator previously described and its main characteristic is that it can provide simultaneous measurement of two polarimeter parameters (i.e. the Faraday rotation and of the Cotton-Mouton effects) as required for ITER, by two phase-only measurements. Other polarimetric methods, based on phase-only and phase-amplitude measurements have been used in various plasma experiments and can be used also for ITER [17-19]. For the purpose of this study it is necessary that a polarization modulated beam is used, but the exact modulation scheme is less important. The "U" method is the simplest way by which a polarization modulated polarimeter can be implemented and we have chosen it for this reason. This polarimetric method has been analysed in detail by Segre using the Mueller calculus [6].

With reference to our scheme of Fig. 1, the signal from the measurement detector, normalized to the incident power, can be written as [20]:

$$I_D = Q_0 + Q_2 \cos(2\omega t + \Phi_2) + Q_4 \sin(4\omega t + \Phi_4)$$

where the coefficients Q_0, Q_2 and Q_4 depend on the plasma but not on the modulation frequency. In a typical tokamak geometry where the polarimetric chords traverse the plasma in a poloidal cross-section, it can be shown that for small plasma effects the two phase shift are given by:

$$\Phi_2 = -\frac{p}{q} W_1 + W_3, \; \Phi_4 = W_3$$

here $p = \cos 2\theta$, $q = -\sin 2\theta$ and θ is the angle of the direction of the linearly polarized radiation at the modulator input, W_3 and W_1 are two quantities related to the Faraday rotation and to the ellipticity change (Cotton-Mouton effect) introduced by the plasma and are given by:

$$W_3 = C_3 \int_L n_e(z) B_z(z)\, dz \quad , \quad W_1 = -C_1 \int_L n_e(z) B_T^2(z) dz$$

where $n_e(z)$ is the electron density, $B_z(z)$ and $B_T(z)$ are the components of the magnetic field parallel and transverse to the probing beam direction, $C_3 = 7.38 \times 10^{-21}\,\mathrm{m^2/T}$, $C_1 = 4.06 \times 10^{-23}\,\mathrm{m^2/T^2}$ (for λ = 118.8 μm) and the integral is taken along the entire plasma propagation path. The information on the parallel and

transverse components of the magnetic field can be obtained by experimentally measuring the two phase shifts Φ_2 and Φ_4. As the method relies entirely on phase measurements, it is in principle independent from the fluctuations of the FIR laser output, as well as to any change of the return beam power due to mechanical vibrations or plasma refraction.

Simulating the plasma by optical wave-plates.

An important issue in this type of experiments is the simulation of the plasma effects by means of a suitable combination of optical elements. In a previous laboratory test of another polarimentric technique (the Segre's "V" method) it has been shown that for a single passage of the FIR beam in the plasma the detected signal can be simulated by the combination of a half-wave plate and a quarter-wave plate, both set with the axis at 45° with respect to the reference direction and rotated togheter around this position [9]. Although the result was derived expressly with reference to the Segre's "V" method, it is also valid for the present technique, provided the orientation of the polarizer in front of the detector is kept to 45° and, more importantly, the two-plate plasma simulator is used in single pass. However in our specific case the plasma simulator would operate in double pass and this method does not work. In fact it can be shown that with a corner-cure retroreflector the changes to the polarization state of the beam during the second pass add up for the plasma but cancel out for any wave-plate pair. This is related to the fact that the Mueller matrix of a plasma and of the two plate combination have different algebraic structures, reflecting the fact that a plasma exhibit circular anisotropy whereas wave-plate have linear anisotropy. For this reason the two-plate simulator cannot be placed in the same position of the plasma as in Fig. 1. For this experiment it has been placed in the return path after the beamsplitter, in front of the analyzer.

Data acquisition and signal processing

Simultaneous measurement of the two phase shifts Φ_2 and Φ_4 can be obtained by using a pair of two-phase lock-in amplifiers, using the signal from the forward beam reflected by the beamsplitter as the phase reference. However two-phase lock-in amplifiers where not available at the RFX laboratory, and therefore we have used a fully digital approach. The plasma simulator was mounted on a PC controlled, step-motor driven rotation stage, and for each angular position, several periods of the signal and reference waveforms have been recorded by a digital oscilloscope. Both signals were numerically processed in the PC and the two phase shifts were recovered by using a signal processing procedure shown in Fig. 4 which efficiently implements the fundamental functions of a two-frequency, two-phase digital lock-in.

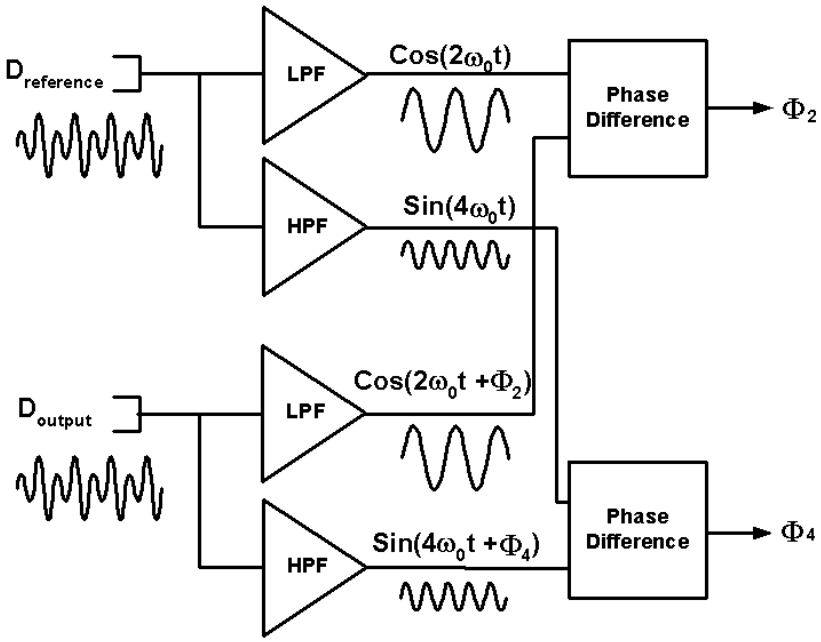

Fig. 4 – Schematic of the digital signal processing for the two phase shift measurement. LPF: low pass filter; HPF: high pass filter.

Experimental results

1) Test of the polarization modulator

The first experiment was a check of the polarization state of the radiation produced by the modulator. This has been measured with the analyzer assembly placed in the beam at the modulator output. No plasma simulator was used. Fig. 5 shows the waveforms detected for various orientations of the linearly polarized beam at the modulator input (corresponding to different values of the ratio p/q), obtained by setting at various angles the axis of the half-wave plate at the modulator input.

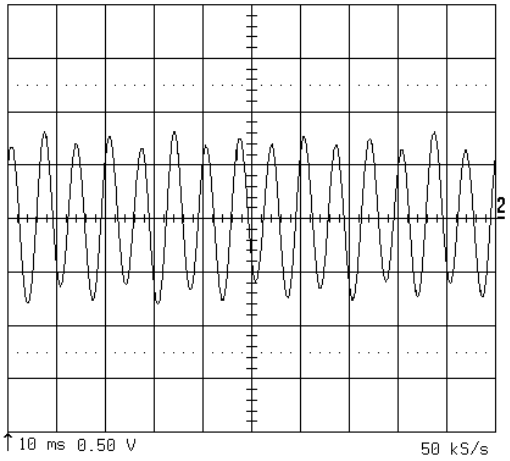

(a) $\lambda/2$ at 0^0

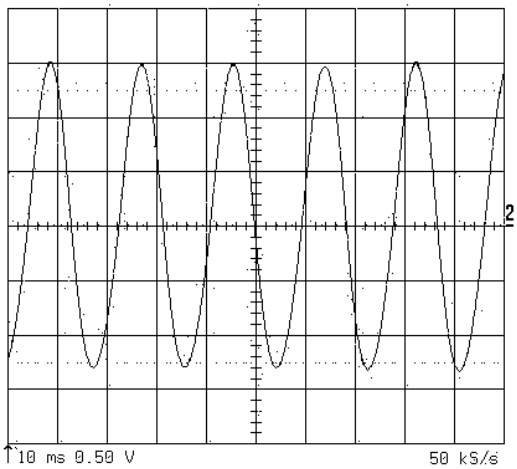

(b) $\lambda/2$ at 22.5^0 mechanical rotation

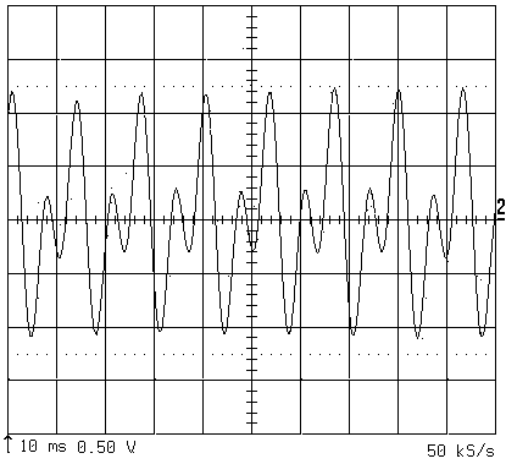

(c) $\lambda/2$ at 5^0 mechanical rotation

Fig. 5 – Checking the modulator output. Waveforms a), b), and c) have been recorded at the modulator output, for three different orientations of the input half-wave plate, corresponding to three different values of the p/q ratio.

These results confirmed that the polarization modulation expected was indeed obtained. They showed that the accuracy of the ratio p/q, whose value is necessary for the interpretation of the phase measurement in terms of plasma parameters, is limited by the angular resolution of the manual rotary mount for the input half-wave plate. The p/q ratio controls also the relative amplitude of the two frequency components and must be determined by a careful calibration procedure. In our case the orientation of the input linear polarization has been nominally set to 10˚ to assure a good balance between the frequency components at 2ω and 4ω in the detected signals. This gives a nominal value of p/q of –2.75. No attempt has been made to determine the p/q ratio to high accuracy.

After the test of the actual polarization modulation obtained, we have carried out a series of different experiments, trying to implement gradually, step-by-step the set-up of Fig. 1.

2) Test of a single pass polarimeter

First we have tested the polarimetric method in a single pass configuration, without the beamline and with no retroreflector, in the simple arrangement of Fig. 6.

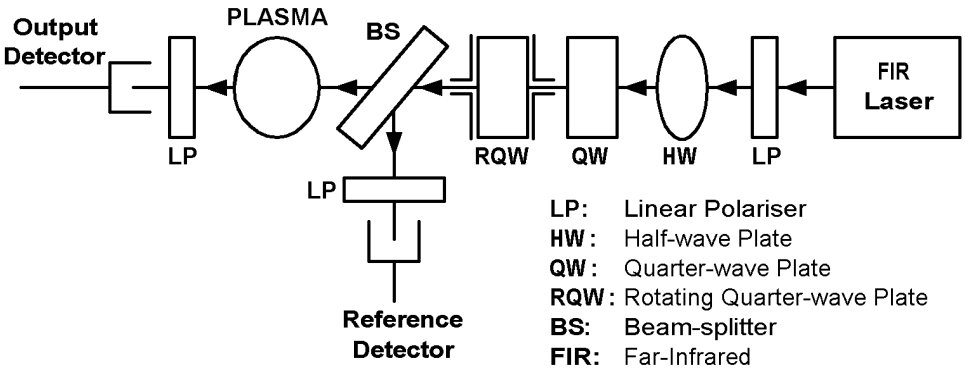

Fig. 6 – Single pass, no beamline polarimeter.

In this case a combination of Faraday rotation and Cotton-Mouton effects were introduced by the plasma simulator located just before the analyzer. The recorded data are shown in Fig 7. Here the two phase signals are repetitively recorded and clearly shows the vertical steps corresponding to small increments (~1˚) of Faraday rotation and ellipticity angles introduced by the plasma simulator. The resolution of these measurements can be estimated by the fluctuations of the recorded phase signal in the flat part of the measured steps and is significantly better than 1˚ .

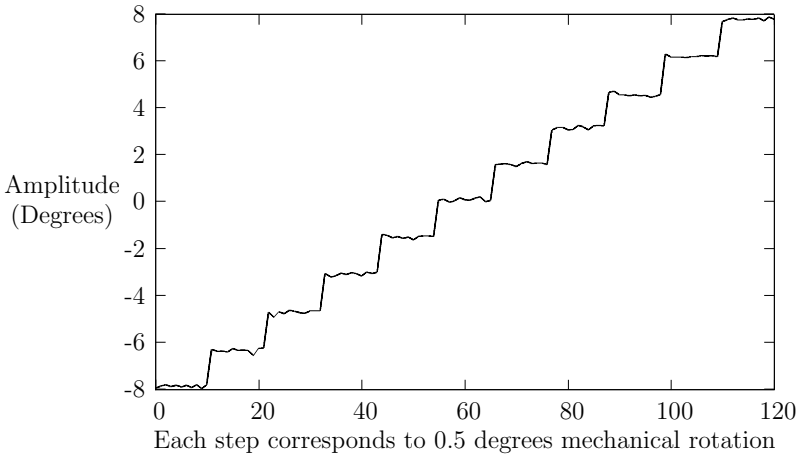

(a) $\Phi_2 = -\frac{p}{q}W_1 + W_3$

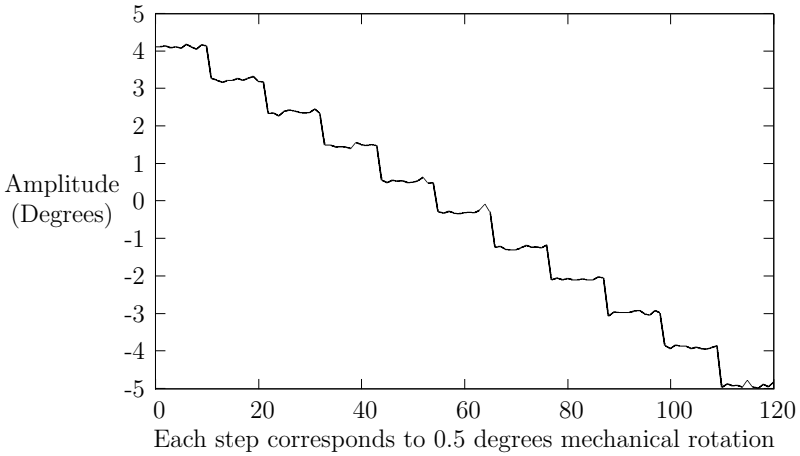

(b) $\Phi_4 = W_3$

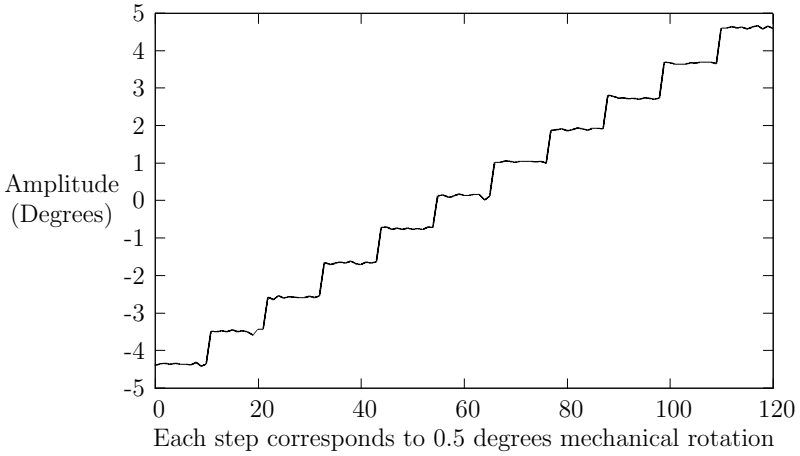

(c) $W_1 = (\Phi_2 - \Phi_4)\frac{-q}{p}$

Fig. 7 – Phase shifts measured in the experiment of Fig. 6. Vertical steps corresponds to phase changes introduced by small angles of Faraday rotation and ellipticity changes.

3) Test of the polarimeter with the corner cube retroreflector

For the following experiment the polarimetric scheme has been modified introducing the corner-cube retroreflector. The experimental layout and the measured data are shown in Figs. 8 and 9:

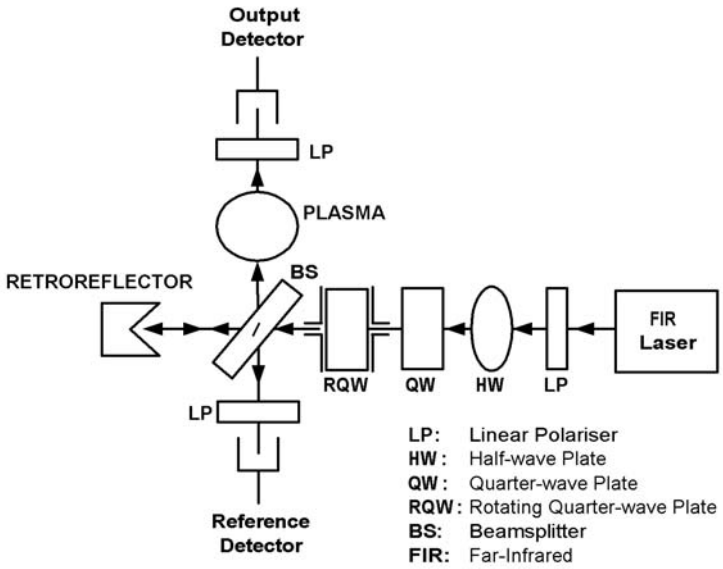

Fig. 8 – Testing the "U-method" with a corner-cube retroreflector.

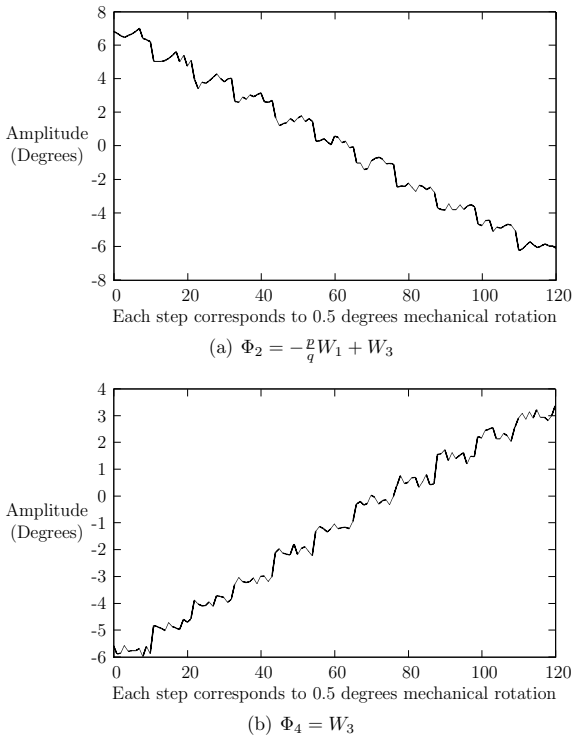

Fig. 9 – Phase shifts measured in the experiment of Fig. 8.

As Fig. 9 shows the noise in the measured data is higher than in the previous experiment and the angular resolution on the measured phase shifts is ~0.5˚. This is due to the higher attenuation of the FIR return beam introduced by the additional reflections in the retroreflector and in the beamsplitter, and, in this case, also to a somewhat lower FIR power output. However the steps in the phase shifts introduced by the plasma simulator are clearly recognized and still measureable.

4) Test of a polarimeter with a single pass in the beamline

In the following experiments, a single passage in the beamline was introduced, without using the retroreflector, accordingly to the scheme of Fig. 10. The measured data are shown in Fig. 11.

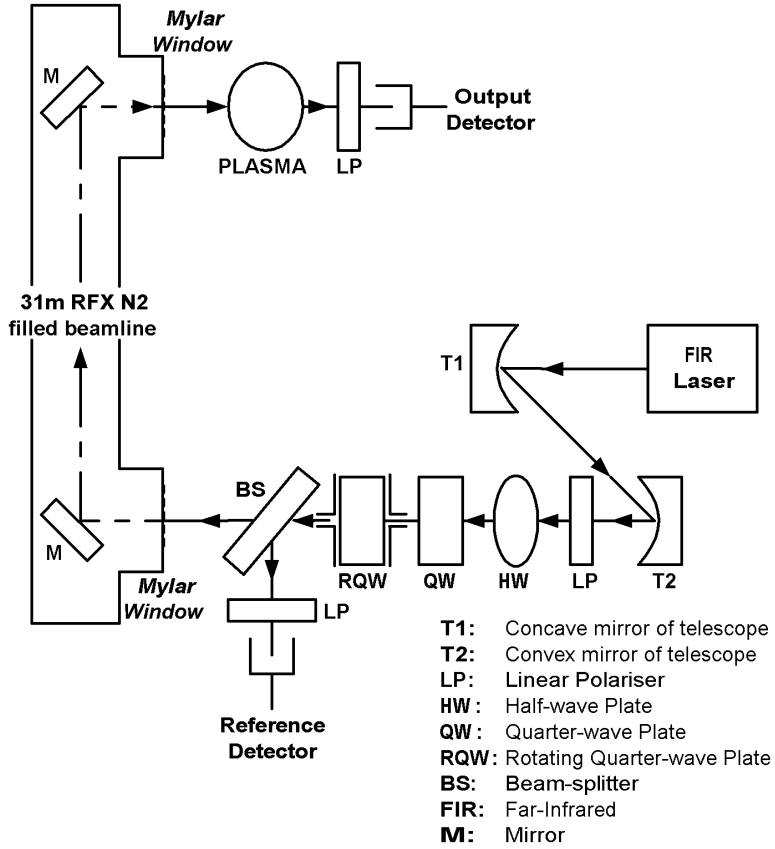

Fig. 10 – Testing the polarimeter in a single pass along the beamline.

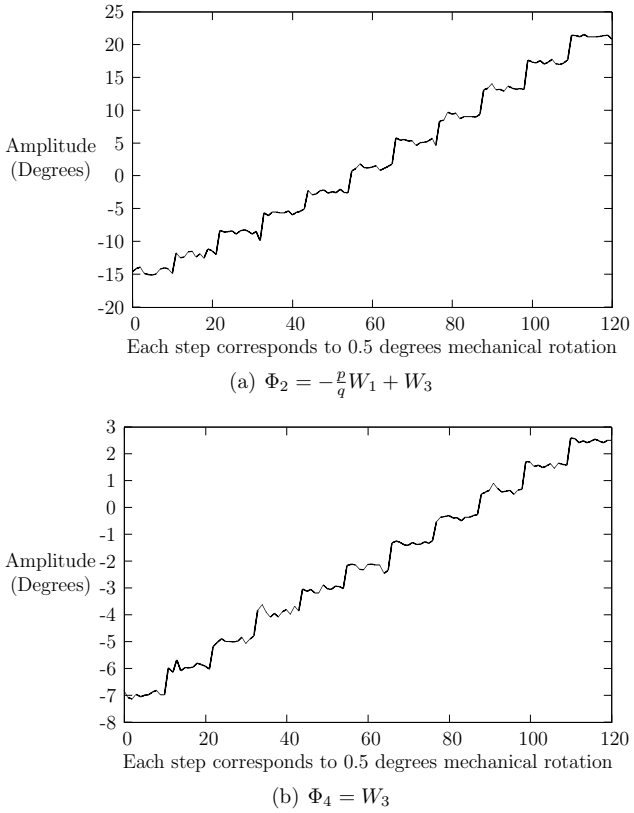

Fig. 11 – Phase shifts measured in the experiment of Fig. 10.

The results are similar to those of the previous experiment, with a somewhat better angular resolution due to the fact that with this configuration a higher FIR power is available at the detector. These results shows that the polarization modulated FIR beam is effectively transported through the beamline with a degree of modulation largely sufficient to perform a good resolution polarimetric measurement, although still without the retroreflector.

5) Test of a polarimeter with a single pass in the beamline and the retroreflector.

Subsequently the corner cube retroreflector was introduced and the scheme in Fig. 12 was tested. Here the modulated beam is first passed through the beamline and the entire polarimeter with the corner-cube retroreflector and the two detectors are located at the end of the beamline. The measured data are shown in Fig. 13.

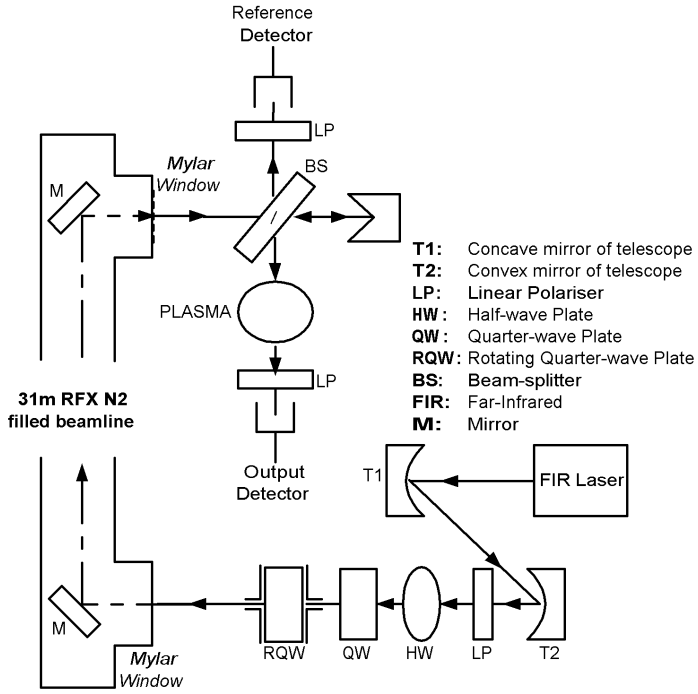

Fig. 12 – Testing the "U-method" with the beamline and a retroreflector

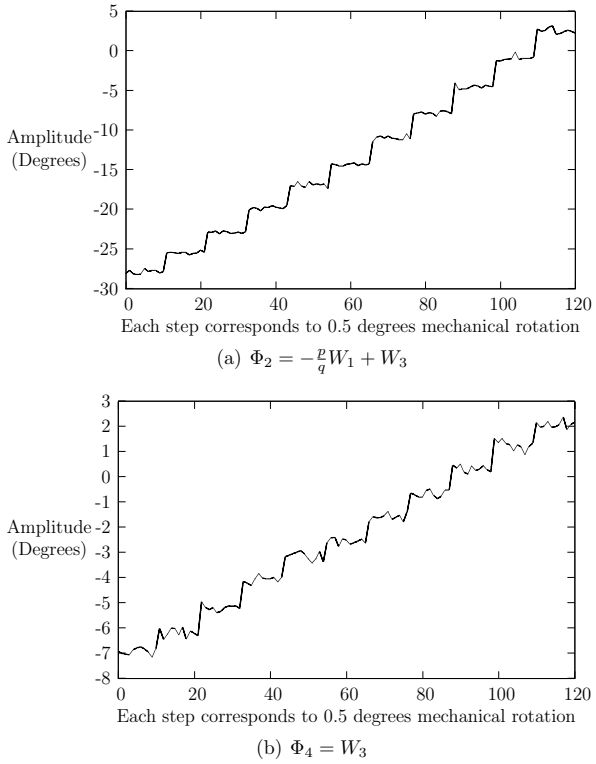

Fig. 13 – Phase shifts measured in the experiment of Fig. 12.

The angular resolution of the phase measurements is ~1˚. Also in this case the changes of the polarization state are measurable, demonstrating that the simulateaneous use of the beamline and the refroreflector does not prevent one from performing polarimetric measurements with sufficient accuracy.

6) Test of a polarimeter with a double pass beamline and retroreflector.

Eventually the last experiment was attempted, with the final polarimeter layout as in Fig 1. However in this case it turned out that it was very difficult to use the RFX beamline in double pass. In spite of a careful alignment of the beam waist with the apex of the corner cube, no return beam could be detected at the beamline input. Part of the problem was due to the fact that in order to assure the proper focalization of the return beam, the refroreflector must be located with high accuracy at the beam waist, i.e. 2.5 m past the beamline output window and the FIR beam is propagated in 5 m of air before reentering the beamline, suffering significant attenuation [2, 21]. Attempts were made to reduce this attenuation by focalizing the FIR beam to a nearer waist by using a shorter focal length parabolic mirror and also a TPX lens, but again the alignment of the return beam into the beamline was not achieved.
However, the previous experiments have clearly demonstrated that a polarimetric measurement in the experimental conditions of ITER is feasible and neither the use

of a long propagation beamline nor the corner cube retroreflection prevents the implementation of a polarization modulated polarimeter. On the other hand the failure of the last experiment showed that the beamline is very critical from the point of view of the alignment of the return beam and it design should take into account small differences in the divergence and mirror centering between the forward and return paths.

The experiment at University College Cork

Parallel experiments on Segre's U-Method were similarly bench-tested at UCC in a single pass arrangement similar to Fig. 6. The results of the UCC experiments demonstrated the same polarimetric method, but with a better time resolution. The main differences between the work carried out in Cork and in Padova were the choice of a higher modulation frequency and a more conventional technique to extract the plasma information from the dual frequency components in the detected signal. A higher modulation frequency corresponding to 250 Hz for the $2\omega_0 / 2\pi$ component and 500Hz for the $4\omega_0 / 2\pi$ was adopted in Cork, ω_0 being the mechanical rotational velocity of the rotating quarter wave-plate. This was made possible by mounting the quarter-wave plate on a high-speed air-bearing spindle, which was driven by a turbine supply. In addition, the spindle was mechanically adapted to generate a reference frequency by passing a visible laser across the face of the rotating spindle and detecting the chopped beam. In this way, the reference signal corresponded to the slower of the composite two-component signal above, namely, $2\omega_0 / 2\pi$.

This composite signal was then fed to two lock-in-amplifiers, each set to measure the phase difference between its input and the reference from the spindle. The front panel switch on one of the lock-in-amplifiers was set to "2F mode" to permit the phase difference to be measured in the $4\omega_0 / 2\pi$ component of the composite input. The output from each lock-in amplifier had a time constant of 10 ms.
In a manner similar to that carried out in Padova, the plasma was simulated using a combination of a half-wave plate and quarter-wave plate mounted in a incremental mechanical rotation stage. The retardation axes of the plates were aligned and set at an angle of 45˚ from the laboratory reference axis. A sequence of small incremental steps about this position simulated small plasma effects, and the gathered data corresponding to the measurement of Φ_2 and Φ_4 was fed to a computer to extract the Faraday rotation angle and Cotton-Mouton effect. Results were similar to those obtained in the Padova experiment, with a resolution of ~1˚ in Faraday rotation and ellipticity angle but a better time resolution of 10 ms, as required for ITER.

Conclusions

This study has demonstrated experimentally for the first time a FIR infrared polarimetric measurement obtained in conditions very similar to those expected in

ITER. In particular it has shown that neither the use of a long propagation path in a metallic mirror beamline nor the use of a corner cube metallic retroreflector introduce fundamental limitations to the possibilitity of simultaneous measurement of Faraday rotation and ellipticiy angle introduced by the ITER plasma. It may be noted that the angular accuracy of ~1˚ obtained in both the Padova and Cork experiments is higher than the 0.2˚ value used for the estimates of the q-profile reconstruction [22]. We point out however that this study was meant to be a test of the polarimeter layout, and not of the specific polarimetric method (i.e. the Segre's U-Method) we used, that is just one of the many methods available for ITER. On the other hand the ~1˚ accuracy obtained is closely related to the polarimetric method and to the characteristics of the experimental apparatus used and we are absolutely confident that it can be improved by increasing the Fir power available at the detectors and the quality of the data processing instrumentation. The 10 ms time resolution, obtained in the Cork experiment is consistent with the ITER diagnostic requirements.

References

[1] A. J. Donne', T. Edlington, E. Jorin, H. R. Koslowski, C. Niewswand, S. E. Segre, P. E. Stott, and C. Walker, Rev. Sci. Instrum., 70, 726 (1999).

[2] A. J. Donne', C. Gil, L. Giudicotti, H. R. Koslowski, P. McCarty, S. Prunty and M. Spillane: "The poloidal polarimeter system for ITER", Final Report for contracts 00/558, 00/559 and 00/560, EFDA (2002).

[3] S. E. Segre, Plasma Phys. Control. Fusion, 38, 883 (1996).

[4] S. E. Segre, Plasma Phys. Control. Fusion, 41, R57 (1999).

[5] M. O'Gorman, E. Zilli, L. Giudicotti, S. L. Prunty, F. Milani, A. Murari, and A. Boboc, Rev. Sci. Instrum., 72, 1063 (2001).

[6] E. Zilli, M. O'Gorman, L. Giudicotti, F. Milani, S. L. Prunty, A. Murari, and A. Boboc, Int. J. Infrared Millim. Waves, 21, 1673 (2000).

[7] D. Elbèze, "Caracterisation des retroreflecteurs"private communication (1999).

[8] V. S. Voitsenya et al., "Measurement of the reflectance of mirrors composing a cube-corner reflector", EFDA Report (2004).

[9] L. Giudicotti, S. L. Prunty, C. Nyhan, E. Bedin, E. Zilli, and L. De Pasqual, Plasma Phys. Control. Fusion, 46, 681 (2004).

[10] "kapton" is the commercial name of a polyimide film produced by DuPont.

[11] D. Elbèze, "Etude pour la calibration des voies réfléchies", private communication (1999).

[12] The metal wire mesh beamsplitter has been designed and manufactured by Prof. Kozlov, of the Academy of Sciences, Institute of General Physics, Moscow, Russia.

[13] M. Nardei and S. L. Prunty, Infrared Phys. Technol. 36, 3, 669-672 (1995)

[14] N. Hodgson and H. Weber, "Optical Resonators", Springer-Verlag, London (1997).

[15] D. Goldstein, "Polarized light, second edition" Dekker, New York (2003)

[16] M. Mujat and A. Dogariu, Appl. Opt. 40, 34-44 (2001).
[17] B. W. Rice, Rev. Sci. Instrum. 63, 5002 (1992).
[18] S. Barry, C. Nieswand, S. L. Prunty, H. Mansfield, and P. O'Leary, Rev. Sci. Instrum. 68, 2037 (1997).
[19] D. L. Brower, L. Zeng, and Y. Jiang, Rev. Sci. Instrum. 68, 419 (1997).
[20] These expressions slighty differ from those in ref. 5 and 6, due to the fact that we use three quarter-wave plates instead of simple quarter-wave plates.
[21] M. Spillane, "Analysis of the propagation characteristics of the optical beamline of the FIR polarimeter on RFX" M.Eng.Sc Thesis, University College Cork, Ireland (2002).
[22] A. J. H. Donné, F. Graswinkel, M. Cavinato, L. Giudicotti, E. Zilli, C. Gil, H.R. Koslowski, P. Mc Carthy, C. Nyhan, S. Prunty and M. Spillane, Rev. Sci. Instrum, 75, 4694 (2004).

APPENDIX

C. GIL 18/04/03

Memo on the semi reflective plates

Introduction

As retroreflectors will be used for the Iter polarimeter, semi reflective plates are needed to separate the incident beam from the reflected beam. We discuss here the positioning of this plate and calculate the efficiency for various materials at 118 microns. The purpose of this memo is to contribute to the discussion, which has started with Dr Giudicotti, who presently is doing experimental tests with some materials at 118 microns.

Set up of the plates

Two configurations can be used:

In the first one the incident beam is transmitted through the plate:

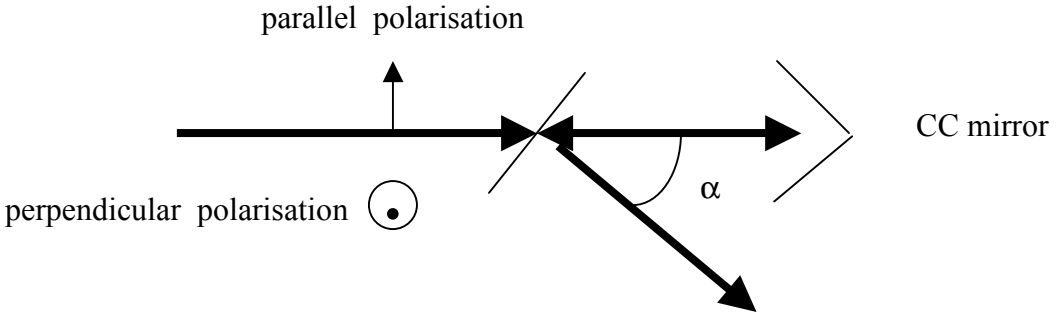

In the second one the incident beam is reflected by the plate:

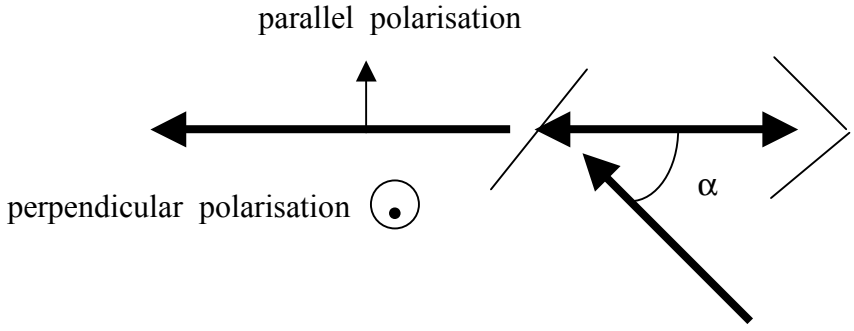

As one can see there are four cases, depending on what is the incident polarisation of the beam:

- case A : incident beam parallel to the incident plan and crossing the plate first.
- case B : incident beam perpendicular to the incident plan and crossing the plate first

- case C : incident beam perpendicular to the incident plan and reflecting on the plate first
- case D : incident beam parallel to the incident plan and reflecting on the plate first

The efficiency of the outcoming beam is the product of the transmission coefficient (T) with the reflection coefficient(R).
E= T*R
Let us call E1 the efficiency, when the output beam is parallel to the incident beam, and E2 the efficiency of the one that is perpendicular.

Reflection and Transmission for various materials

We discuss the efficiency for three materials (quartz,mylar,kapton) and different thickness versus transmission and reflection coefficients.

An other important parameter is the angle of the plate. Two cases are examined. The first one is small angle case, say 7°, which allows to separate the reflected beam from the incident one in approximately 50 cm . The second one is the Brewster angle (60°), which allows optimising one reflected component.

One needs to know their ordinary and extraordinary index and absorption coefficients at 118 microns:

	O index	O absorption (cm-1)	X index	X absorption (cm-1)	Reference
Natural Quartz	2.1204	.63	2.1694	.47	(1)
Mylar	1.7	40	1.7	40	(2)
Kapton	1.793	8.3	1.793	8.3	(2)

Ref 1 : Veron : Submillimeter Interferometry of high density plasmas, in Infrared and millimetre waves, vol 2 , edited by K Button ,Academic press 1979
Ref 2 : Applied Optics June 1975 Vol 14 N°6 p 1335

Then one can calculate transmission and reflection of a parallel face plate versus its thickness and the angle of incidence. I have my own electromagnetic matlab code, but I think it can be understood in studying ref 3
Ref 3 : Veron , appl optics 1986 vol 25 n°5 p621
My own code has been tested a lot of times and appears to fit very well the experimental tests that we have done in the past.

Results

Case A: incident beam parallel to the incident plane and crossing the plate first.

Plate angle (degree)	7					60				
Output beam polarisation	Parallel to the incident plan			Perp.		Parallel to the incident plan			Perp.	
	T	R	E1	R	E2	T	R	E1	R	E2
Mylar 18 µm	.721	.219	.163	.226	.158		0			
Kapton 25 µm	.829	.151	.125	.156	.126		0			
Kapton 50 µm	.703	.263	**.185**	.270	**.190**		0			
Quartz 2012 µm	.736	.137	.101	.397	.292		0			
Quartz 2423 µm	.532	.357	**.190**	.392	**.209**		0			

Case B : incident beam perpendicular to the incident plan and crossing the plate first.

Plate angle (degree)	7					60				
Output beam polarisation	Parallel to the incident plan			Perp.		Parallel to the incident plan			Perp.	
	T	R	E1	R	E2	T	R	E1	R	E2
Mylar 18 µm	.715	.219	.156	.226	.161		0			
Kapton 25 µm	.825	.151	.125	.156	.129		0			
Kapton 50 µm	.695	.263	**.185**	.270	**.188**		0			
Quartz 2012 µm	.534	.137	.07	.397	.212		0			
Quartz 2423 µm	.526	.357	**.188**	.392	**.206**		0			

Case C incident beam perpendicular to the incident plan and reflecting the plate first.

Plate angle (degree)	7					60				
Output beam polarisation	Parallel to the incident plan			Perp.		Parallel to the incident plan			Perp.	
	R	T	E1	T	E2	R	T	E1	T	E2
Mylar 18 µm	.226	.721	.163	.715	.161	.585	.920	.538	.36	.211
Kapton 25 µm	.156	.829	.130	.825	.129	.595	.976	**.581**	.392	**.233**
Kapton 50 µm	.270	.703	**.190**	.695	**.188**	.569	.953	.543	.395	.225
Quartz 2012 µm	.397	.736	**.292**	.534	**.212**	.740	.857	.634	.213	.157
Quartz 2423 µm	.392	.532	.209	.523	.205	.611	.843	**.515**	.306	**.187**

Case D: incident beam parallel to the incident plane and crossing the plate first.

Plate angle (degree)	7					60				
Output beam polarisation	Parallel to the incident plan			Perp.		Parallel to the incident plan			Perp.	
	R	T	E1	T	E2	R	T	E1	T	E2
Mylar 18 µm	.219	.721	.158	.715	.156	0				
Kapton 25 µm	.151	.829	.125	.825	.125	0				
Kapton 50 µm	.263	.703	**.185**	.693	**.183**	0				
Quartz 2012 µm	.137	.736	.100	.534	.07	0				
Quartz 2423 µm	.357	.532	**.19**	.526	**.188**	0				

Discussion:

- One can see that the efficiency E of a 50 micron Kapton plate is very similar to the one of an optimised natural quartz plate. The expected efficiency always turns around 20%, excepted one case in C where one efficiency reaches 30 and 60%.

-This efficiency seems to be good enough for the diagnostic. Especially if we consider that the probe beam will be mixed with a frequency shifted beam. Thus, on the detector, the signal will be proportional to the product of the two beam mixed amplitudes. As the calculated reflection, transmission and efficiency terms are intensity parameters, the decrease, due to the plate, on the detector will be proportional to the square of the efficiency E. That means a decrease of only 55% on the detector signal.

-The choice of material:

Kapton is a very easy material to use. The visible reflection coefficient of an alignment beam is good enough. The surface quality is also good enough for visible alignment. The Infrared reflection is not very sensitive to a change of the incident angle. It is inexpensive. It can be sensitive to phonic perturbations. Thus the plate boxes must be isolated from any noise source.

- Mylar is less good in term of efficiency, although quite similar, and very cheap.
- Natural quartz is quite expensive but good in efficiency. As the plates are thick, there are two disadvantages. One is that the reflection coefficient changes very fast versus the incident angle. If the following mirrors are too near the plates, some errors of alignments can occur, due to the change of reflectivity versus the angle. The other problem is that a visible beam is reflected on the two interfaces of the plates and a double beam is created, which can lead to mistakes.
-

-Small or Brewster angle.

The efficiency of a Brewster angle is better than the small angle, at least, for the polarisation component which has turned because of the Faraday effect: 58% instead of 20 %

The disadvantages of this configuration are: If no calibration system is settled between the Corner cube and the plate (remember that half wavelength plates cannot be used. Only rotating and removable grids could be used for calibration) one has to correct the measured rotation of polarisation, in taking in account the reflection or transmission coefficients. We have shown (SOFT 2000) that errors on the angle of the plate are far less important when the angle of the plate is small, because, in this configuration ,the two coefficients are very similar)

Conclusion : I think that the gain of power in Brewster configuration is not worth

-Crossing first the plate or reflection first.

In term of efficiency , it is very similar. The advantage of crossing first is that the incoming infrared (or visible) beam on the CC is stronger in this configuration and will be easier to measure with intermediate detectors.

- Incident polarisation : Nearly no effect. May be it is better to have the strongest reflection coefficient on the polarisation component which has turned.

Annex IV (CEA): Experimental study of plasma exposure of a corner-cube reflector

COMMISSARIAT A L'ENERGIE ATOMIQUE

Département de Recherches sur la Fusion Contrôlée
Service Chauffage et Confinement du Plasma

Association EURATOM-CEA

Téléphone : (0) 4 42 25 6222
Fax : (0) 4 42 25 6233
Email : dirsccp@drfc.cad.cea.fr

CEA/CADARACHE F-13108 ST-PAUL-LEZ-DURANCE

Activité	**DIAGNOSTICS**
Nature	**NOTE DE TRAVAIL**
Référence	**DIAG/NTT 2005-003**
Titre	**Final report of the EFDA TWP2002 Contract 02-1003** **Support to the ITER Diagnostic Design : Polarimetry** **Experimental study of plasma exposure of a corner cube reflector**
Auteur(s)	Christophe Gil

Résumé	For this contract, the due specific CEA contributions were the following analysis: i) Characterize the change of optical performance of a corner cube reflector exposed to plasma. ii) Interpret the observed changes in the optical performance in terms of plasma processes occurring at the reflecting surfaces. The first part of this report deals with these two specific tasks As a contribution to the polarimeter feasibility study , the second part of this report is a memo on the semi-reflective plates , which will be needed to split and recombine the FIR beams.
Annexe(s)	

Destinataires :

B. Echard, D. Elbèze, J Philip, L Toulouse, C Desgranges, C Brosset, M Lipa, B Schunke
P Magaud, christian.ingesson@efda.org

dir. SCCP, dir. SIPP

Visa Rédacteur	Visa Vérificateur	Visa Qualité, Structure	Visa Emetteur
C. Gil Date :	Date :	Date :	A. Bécoulet

FIRST PART : RETROREFLECTOR STUDY

Introduction

The previous contracts for the definition of the ITER poloïdal polarimeter system [1] led to the proposal of having diagnosing 119 micron wavelength far infrared beams that would cross the plasma from an external port to the inner blanket, where corner cube inner reflectors (CC) mirrors could reflect them back to the entering port.
These inner mirrors would therefore be exposed to the wall conditioning and the plasmas. Their induced deterioration is important to evaluate and the impact on the characteristic of the reflection must be appreciated.
The aim of this work was to gain experience, in the FIR wavelength range, on the change of reflectivity of a CC mirror when it has been exposed during an experimental campaign to long duration Tore Supra plasmas.
It has been done in parallel to the EFDA contract TW2-TPDS-DIADEV-D02 [2], which studied the changes in shape and reflectivity of flat mirrors of different metals. They have been similarly exposed during the same experimental campaign. For polarimetry, this study deals with two particularities, which are the very long used wavelength of the incident beam and the geometry of the CC mirror, formed by three contiguous perpendicularly oriented faces.

Mounting of the CC mirror in the TS vessel

At the beginning of the year 2003, a special first wall panel has been installed in the Tore Supra vessel. This panel had been designed for the future FIR interferopolarimeter. It is a double embedded stainless steel sheet, which is cooled by 30 bars water at 130°C (fig 1). Through five holes, some 80 mm diameter holders have been welded (fig 2). As these holders are in CuCrZr alloy for better thermal conduction, an intermediate Nickel ring is inserted for good welding. The welding between steel and nickel is TIG and between nickel and copper is made by electron beam.
The CC mirror is screwed on the holder (fig 3). A soft compliant 0.2 mm thick layer (PAPYEX) is inserted between the mirrors and the ring holder and the base structure, in order to enhance the heat transfer to the cooling panel.

The characteristics of the mirror, given by the manufacturer, are the following:

- The 3 faces are dug by spark erosion in a bulk CuCrZr material (photo fig 4).
- The optical diameter is 50 mm
- Sharpness of the interfaces : less than 50 microns radius.
- Flatness of the mirror surfaces : peak to peak better than 25 microns
- Roughness : 0.4 Ra by hand polishing

One can see on figure 5 the panel with the mirrors in the TS vessel. They are situated roughly 140 mm behind the last magnetic closed surface. The CC is at the lowest position and is 57 mm below the equatorial plan of the tokamak (-3.6° angle from the centre of the vessel).

As a reference, two plane CuCrZr polished mirrors, which have a diameter of 80 mm have been also installed. One is the fourth from the bottom at a vertical position of 347 mm from the equatorial plan (22.7°) and the other is situated higher at 819 mm (65.0°)
Notice that there are two other holders with six metallic 20 mm of diameter samples, which are made of copper, stainless steel and molybdenum and are fixed at 7.6° and 15.4° (fig 5). The purpose of these samples was to study the change of reflectivity after one year of plasma exposure in the frame of the other EFDA contract [2]. But the results will be compared to the CC ones as well.

Exposure of the CC during the 2003 and 2004 campaigns

The mirrors have been recovered in April 2004, after more than one year of plasma campaign. An analysis of the conditions of plasma exposure and wall conditioning has been made in the TW2-TPDS-DIADEV-D02 report [2] and is reproduced thereafter:
" During this period roughly 1400 plasma pulses (mainly D_2) of more than Ip = 200 kA (n_{e0} ~2-4 10^{19} m^{-3}) have been performed with a cumulated pulse length of ~26000s (7h10) corresponding to an average pulse length of ~18 s. The accumulation of injected energy in TS between March 2003 and April 2004 was roughly 37 Gigajoules (GJ) composed of ~13 GJ Ohmic, ~22 GJ LH and ~2 GJ FCI . The average heating power per plasma pulse was therefore about 1.43 MW. The cumulated radiated average energy wall load would be ~18 kJ/cm² if ones take into account a typical value of radiated plasma power loss of about

40 %.
In addition, wall condition procedures, alternating with plasma operation, have been performed during this exposure time :

Glow discharges He:	361h 59 min (cumulated)
Glow discharges D_2:	606h 18 min (cumulated)
Boronisation:	13h 40 min (cumulated)

Besides minor leaks, there has been a major water leak of an actively cooled in-vessel component in September 2003, after 177 h of D_2 and 108 h of cumulated He glow discharges. Minor water leaks on RF antenna structures appeared also during March 2004.
The final TS operation time, before mirror recovery, lasted over 2495 s of cumulated plasma operation (including very long discharges over pulse length of more than 100 seconds), followed by a final 6,5 h He Glow discharge and an additional 85 s of plasma operation.
Baking cycles of the vacuum vessel structure were performed at temperatures around 200 °C. It should be mentioned that in-vessel components in TS are cooled/baked by a pressurized hot water circuit operating in the range of 120-200 °C at roughly 30 bars. As cooled in-vessel components are constructed of different materials, the AVT (all volatile treatment) water chemistry has been adjusted to cope with this requirements. The ph value of the liquid/vapor mixture during leakage in the vacuum vessel can be assumed to be around 7.0. "

In the TW2-TPDS-DIADEV-D02 report, the surface temperature of the mirrors has been also evaluated:
" 2D- thermohydraulic finite element calculations of the mirror sample assemblies have been performed using the Castem 2000 code. It showed for the different mirror samples a maximum temperature rise of roughly 15 °C (Twater = 120 °C) for a typical "Gigajoule" operation scenario with an expected absorbed heat flux of ~0.011 MW/m² (~1 MW radiated plasma power loss) during a pulse length of 360s. The initial assembly temperature is reached after 300 s following the plasma pulse. Therefore the maximum mirror exposure temperature during operation can be taken to be around 150 °C "

This 150°C temperature can be set as a good approximation for the faces of the CC because even if they are partially hidden from the total plasma radiation, the conductivity of the copper is great enough to equalize the temperature between the surface and the faces.

Surface modifications of the mirrors after exposure

One of the important information that is expected to be given by plasma exposure of mirrors, is to know how the surfaces change. Deposition and erosion by neutral atoms or ions are in competition to increase or decrease the depth of the mirror .
On figure 6 one can see the surface look of the lower fixed bulk plane CuCrZr mirror after plasma exposure. There is no trace of deposition on it but a dull appearance, due to erosion. Notice that on the copper 20 mm diameter samples that have been similarly exposed, a 2.6 micron erosion has been measured [2]. On the contrary, the upper fixed mirror has a dark aspect which may due to deposition. As the corner cube geometry leads to partially hide the faces from the plasma , the 2.6 micron erosion may be considered as an upper plausible limit.
On the exposed CC (fig 7), one can also find a dull surface outside the 50 mm diameter and even 3 dull zones on the 3 faces of the CC, corresponding to eroded zones. But there is in the centre of the CC a large dark triangular zone , which corresponds to a deposition zone. A detailed photo of one face can be seen on figure 8

The analysis of the deposition would need to cut the CC. This is not possible because it is intended to continue the analysis of the optical parameters of the CC. Thus only qualitative remarks can be done :

- On the 3 faces, the geometry of the deposition is the same. This symmetry , independent from the magnetic field lines, leads to conclude that the plasma confined ion interaction with the CC is not dominating in the mechanism of surface change. This can be explained because the mirrors are situated 140 mm away from the last magnetic surface. Thus only charge exchange fast neutrals atoms or non confined wall conditioning ions are supposed to significantly interact with the CC to erode it. On the contrary, the slow atoms, which are generated during the plasma, could deposit.
- As discussed in reference 2 , because of the complicated sequence of events that happened during the campaign, it is hard to determine which has been the determining erosion parameter- plasma or wall conditioning. In future measurements it would be interesting to have some reference samples equipped with shutters which could be opened only during wall conditioning to compare with the permanently exposed mirrors.

- On the detailed photo (fig8) , one can clearly see that deposited matter has grown in the shadow of the edge that is situated in front of the face. Interference layers can be seen and imply that the deposition layer gradually grows toward the centre of the CC.

Some hypothesis can be given to explain the growth of a deposited layer in the centre of the CC

- In the inner part of the CC, the eroding flux is low because the solid angle is reduced by the shadowing effect of the edge. On the contrary, on the external part, the total eroding flux is sufficient to remove the deposited layers.
- In the inner part, the efficiency of the eroding flux is lower because the ejected atoms can redeposit on the faces, due to the great depth of the CC.

To explain the difference of look between the two plane mirrors (one dark and the other eroded), one hypothesis is that the eroding flux is lower in the upper part of the vessel. This asymmetry still needs to be explained because not only the plasma ions are involved in the erosion , but the wall conditioning ones as well.

Quantitative simulations taking into account all the above described mechanisms would be interesting to explain the layers of the Tore Supra CC and to predict the behaviour of the CC in ITER. Further experiments with shutter equipped mirrors could help to confirm the simulations.

Reflectivity measurement

Before the plasma exposure, the reflectivity of the CC and the plane mirror has been measured at 118 microns, using the Tore Supra H2O laser facility.
One can see a scheme of the experimental set up on figure 9: A semi reflective plate that is made of a plastic film of Mylar is used to send the FIR beam to the CC mirror. The reflected beam goes back through the Mylar and is then focused on a pyroelectric detector which measures the intensity of the reflected beam. Note on the table 2 below the figure 9 that the gaussian beam diameter is around 20 mm on the optical element and 0.6 mm on the detector.
The copper CC and plane mirrors were compared with a reference dielectric plane mirror. Alternatively, one mirror and next its reference dielectric mirror were mounted, and the intensity of the beam measured. At every change of mirror, the beam was realigned on the detector. The reflectivity is considered as the ratio of the two intensities. Due to the uncertainty of the measure, which we will discuss after, no significant difference of reflectivity was observed.

After the plasma campaign, the reflectivity of the exposed mirrors has been measured. It has been compared with various reference mirrors that had not been exposed to plasma.

Exposed mirror	Intensity A. U.	Reference mirror Not exposed	Intensity A. U.	Reflectivity %
Copper CC	5.55	Copper CC	5.9	94
Copper CC	5.5	Dielectric CC	6.0	92.5
Copper Plane mirror	7.9	Dielectric plane mirror	7.6	103.4

Table 1 : Experimental results of reflectivity measurements

Notice that the measure of reflectivity of the 20 mm plane samples, which is reported in the other EFDA contract [2], also showed no significant change of reflectivity (reflectivity between 96 and 101%)

Discussion on the results of table 1.
We shall discuss now on the significance of these results. If there is a slight loss on both of the measures of CC reflectivity, the observed scattering of the results on the plane mirrors leads to conclude that the error bar may be up to 10% .
Such big uncertainties come from the set up of the experiment itself, which has some defects:
-Though the output power of the laser is quite stable, there is a lack of a second pyroelectric detector to monitor the power.

-All the experiments have been done in a dried air box , to avoid absorption of the FIR beam. But at every change of mirrors the box must be opened, which induces a small variation of dried air and the time recovery can be very hazardous .
- The pyroelectric detector is quite noisy and would need a better electronic to analyse such small changes. Moreover, this kind of detector is very sensitive with the temperature that is not controlled in this experiment.
- When changing the mirror, the need to realign may introduce some errors in the measure.

All these minor defects can add themselves and lead only to conclude that no big changes of reflectivity have been found. If there are any, they are small and must be confirmed on a more adapted other experimental set up. Unfortunately, our TS facility cannot easily be changed because it has been designed specifically for the plasma diagnostic in an overcrowded space.

Some recommendations can be done for improving the relevance for ITER. The measures would need to respect the following conditions:

- The size of the gaussian beam on the CC must be around 12 mm as proposed on ITER. On TS it was 20 mm . Spurious effects due to changes of the interfaces of the faces can be more important with a smaller beam.
- On ITER the first focus mirror is situated more than 5 metres away from the CC . On TS the first focus is much nearer the CC. It would be interesting to have a longer distance in a reflective experimental set up, in order to be able to estimate a possible broadening of the reflected gaussian beam when the CC is polluted.
- For the ITER polarimeter , it is very important to know if there is a depolarisation of the beam when the CC has changed. It has not been possible on TS to measure the depolarisation effect of the exposed CC because of the lack of space in the set up , where no rotating grid could be inserted.
- As the copper erosion rate is high compared to tungsten and molybdenum, which are the potential materials for the ITER CC, it is interesting to do experiment with copper CC because the erosion mechanisms can be seen even on smaller plasma devices than ITER. Nevertheless, as a comparison , it would be interesting to expose Mo or W CC as well and compare the changes of reflectivity.

Comparison with the theory of reflectivity

To interpret the reflection results, one needs to know the average roughness, in order to compare with the theoretical Bennett' formula [3]:

$$R = R_0 \exp[-(4\pi d)^2 / \lambda^2]$$

Where R_0 is the ideal reflectivity, λ is the wavelength and d the average roughness.

With our one piece made CC it seems difficult to cut one face for analysis without damaging it.
We only can refer from the results of the analysis of flat copper sample of reference 2 , which are 2.6 micron width erosion and around 50nm of roughness . Due to the geometry of the CC , one can assume that the erosion has not been as homogeneous as on a flat sample. Therefore the average roughness of the exposed CC may be higher than the measured 50nm but at least less than 2.6 microns.
It is even more difficult to estimate the width of the deposited layer, but as one can see interference irisation (fig 8), the width must be in the range of the visible , say the micron.
From the Bennett formula, the expected reflectivity is thus situated between 92% (2.6 micron roughness) and 99.99% (50nm). One can see that the experimental results are compatible with the theory.

Nevertheless, it would be interesting to redo the experiment with an assembled face made CC , in order to be able to analyse the roughness on each face separately after the plasma campaign.

Conclusions and prospects

During one year of TS experimental campaign , copper alloy CC and plane mirrors have been directly exposed to vessel conditioning and plasmas.

Their surface looks have changed . Evidence of erosion on the plane mirror and on the external parts of the CC, and deposition in the centre of the CC have been seen. But more analysis would have to be done to characterise the changes and in particular experiments to dissociate the wall conditioning influence from the plasma one. In parallel, simulations of the mechanisms of erosion- deposition induced both by plasma and wall conditioning, including the effects of the CC geometry, would be interesting in order to be able to extrapolate to the ITER CC .

The measurements of the reflectivity of the CC that have been done at 118 microns on TS, show no great decrease of reflectivity , less than 10% for the CC and not measurable for the plane mirror. The results seem compatible with the theoretical values predicted by the estimated roughness. But they can only be considered as a rough estimation because the experimental set up on TS is not adapted to measure small changes. A more precise experiment , including effect of long distance beam changes and depolarisation and surfaces analysis must be foreseen. This is why 119 microns reflectivity measurements of the plane mirrors have started at the RFX laboratory of Padova to confirm these results.

As there have been such small changes both on the looks and on the reflectivity of the mirrors in a one year campaign , it is interesting to have more significant data with longer exposures . For the future TS campaigns , 5 CC will be exposed to plasmas and the analysis of their changes will be of interest to complete this preliminary work.

References

[1] A.J.H Donné, C.Gil, L. Giudicotti, H.R. Koslowski, .P.Mc Carthy, S.Prunty, M. Spillane, 'The poloidal polarimeter system for ITER', Final report on EFDA Contracts 00-558,00-559 and 00-560,May 2002
[2] 11. M. Lipa, B. Schunke, Ch. Gil et al., First mirror study in Tore Supra, EFDA ref. TW2-TPDS-DIADEV-D02, Final report, December 2004.
[3]H. E Bennett ,JOSA,53,1389(1963)

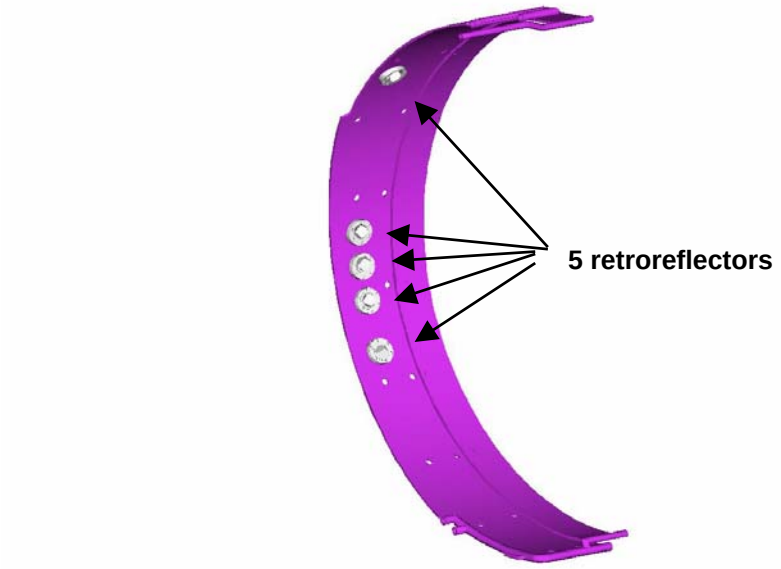

Figure 1 :Drawing of the PEI stainless steel panel with five retroreflectors

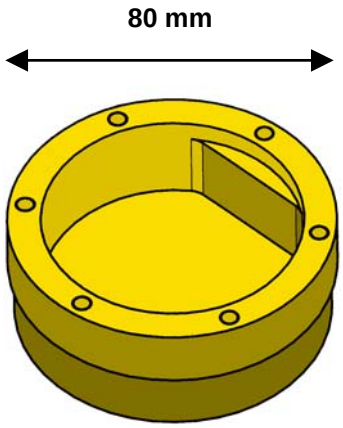

Figure 2 Drawing of the CuCrZr holder

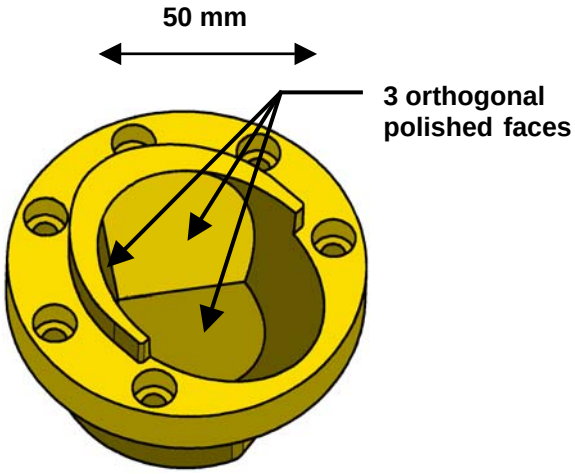

Figure 3 : Drawing of the CC mirror

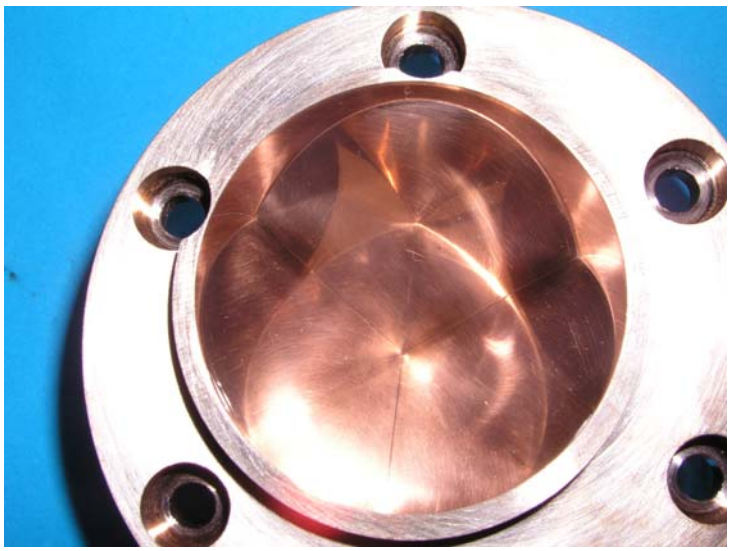

Figure 4 : Photo of the polished faces of the CC before plasma exposure

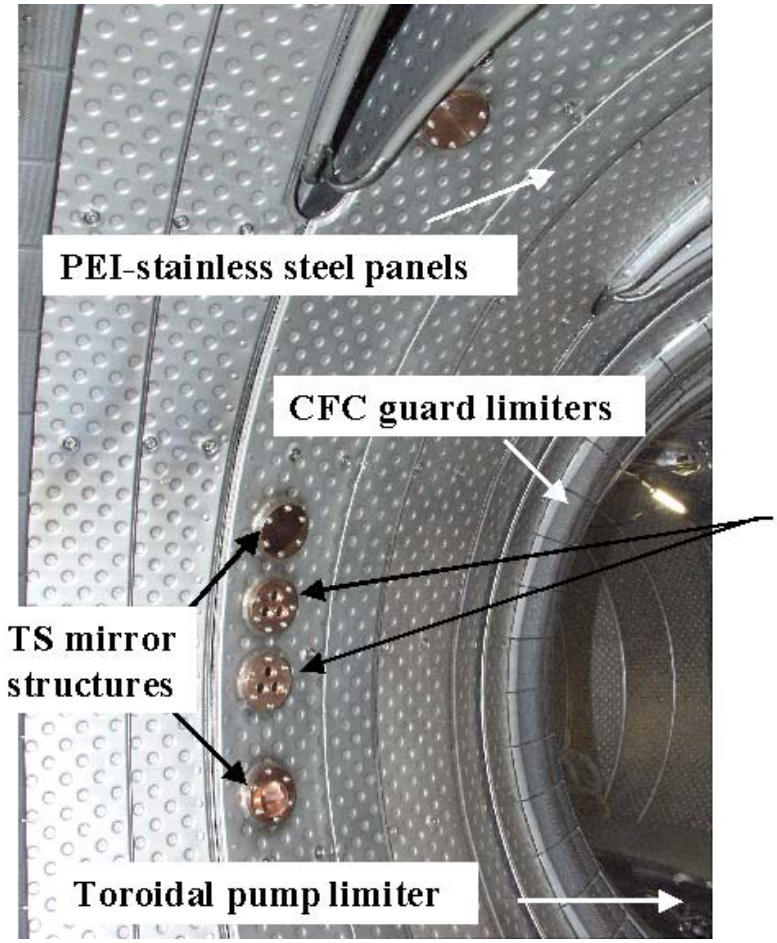

Figure 5 Panel with the mirrors installed in TS
The CC mirror is the first from the bottom , nearly on the equatorial plan
The reference plane mirrors are the forth and fifth from the bottom.

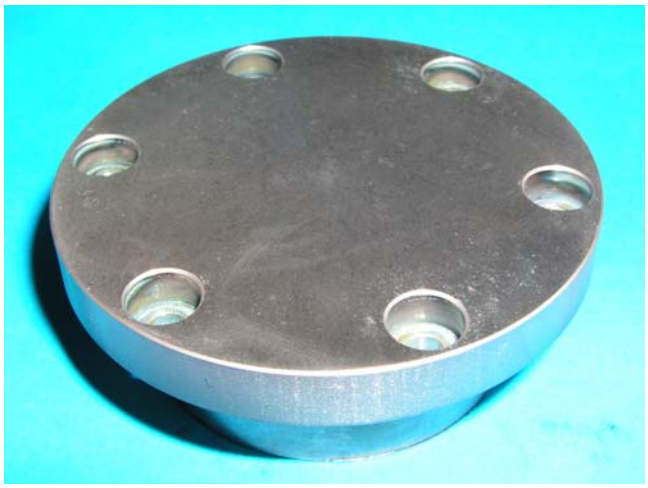

Figure 6 Surface view of the flat low fixed CuCrZr mirror , which was initially polished at λ, after plasma exposure

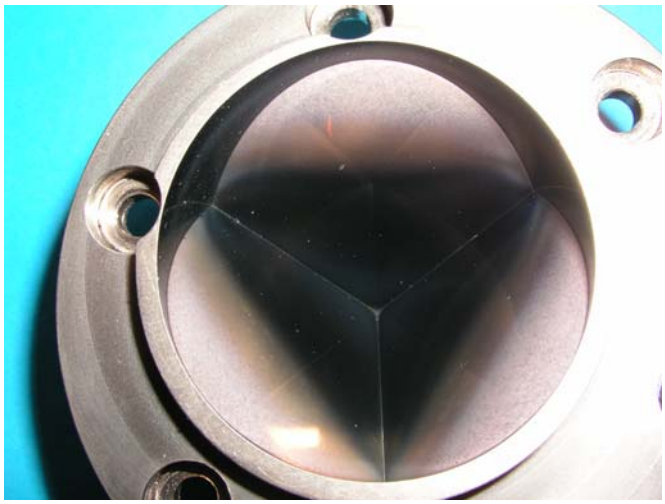

Figure 7 Surface view of the CC mirror after plasma exposure . The dark triangle is due to deposition of a material that has not yet been analysed

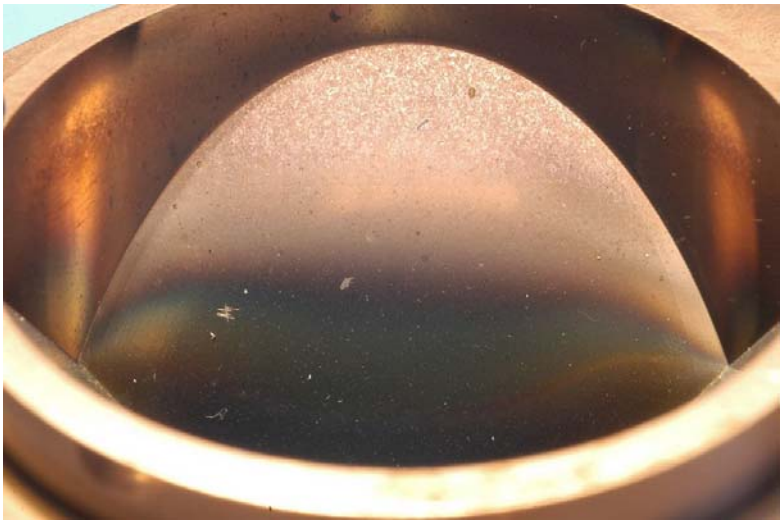

Figure 8 Detail of one face of the CC

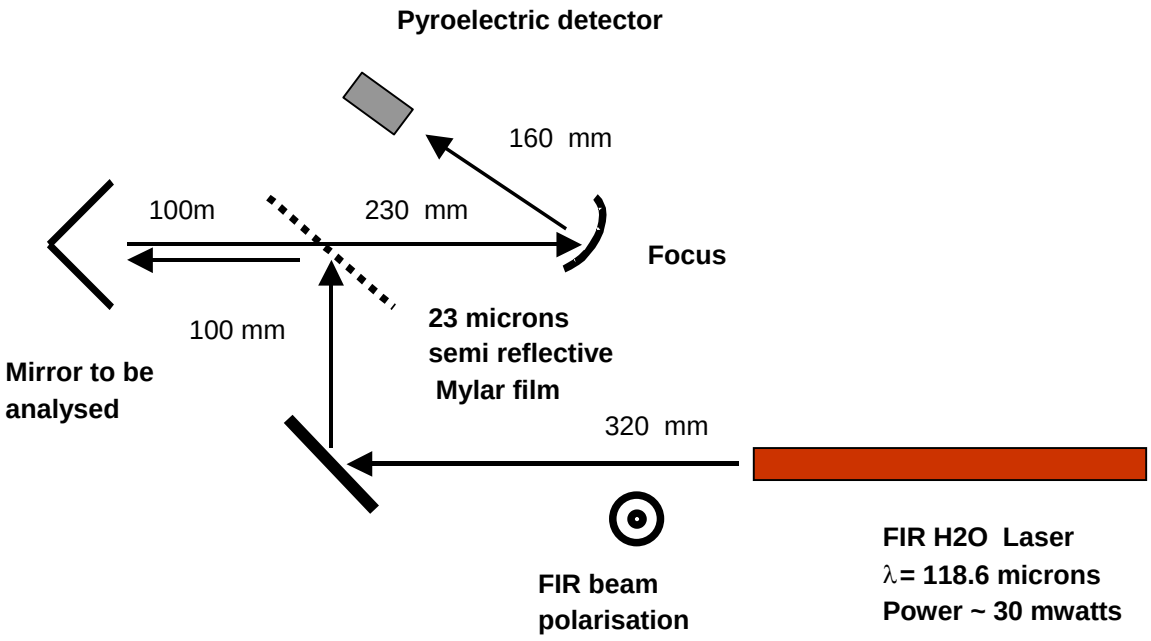

Figure 9 : Scheme of the experimental set up for the reflectivity measurements

	Diameter of the optical components (mm)	1/e diameter of the gaussian beam (mm)
Laser output	**50**	**19.5**
CC mirror	**50**	**19.7**
Mylar	**60**	**19.7**
Focus mirror	**60**	**19.7**
Detector	**2**	**0.6**

Table 2 : Characteristics of the optics of the experimental set up

SECOND PART: Memo on the semi reflective plates

Introduction

As retroreflectors will be used for the ITER polarimeter, semi reflective plates are needed to separate the incident beam from the reflected beam. We discuss here the positioning of this plate and calculate the efficiency for various materials at 118 microns.

Set up of the plates

Two configurations can be used:

In the first one the incident beam is transmitted through the plate:

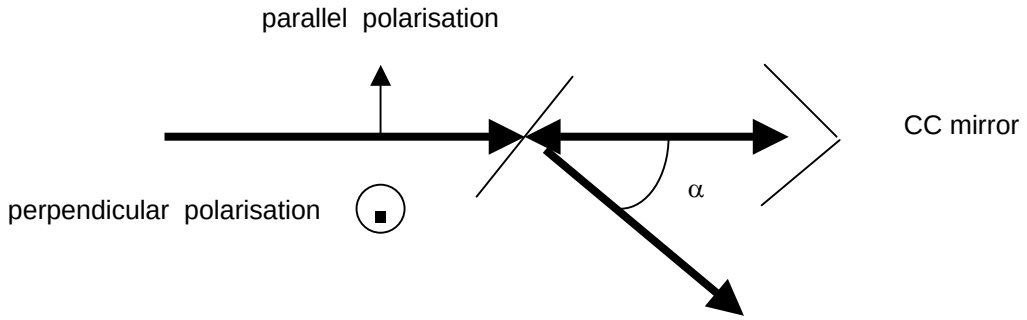

In the second one the incident beam is reflected by the plate:

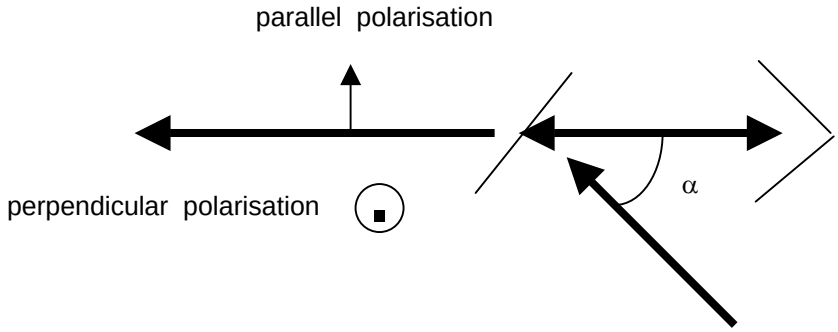

As one can see there are four cases, depending on what is the incident polarisation of the beam:

- case A : incident beam parallel to the incident plan and crossing the plate first.
- case B : incident beam perpendicular to the incident plan and crossing the plate first
- case C : incident beam perpendicular to the incident plan and reflecting on the plate first
- case D : incident beam parallel to the incident plan and reflecting on the plate first

The efficiency of the out coming beam is the product of the transmission coefficient (T) with the reflection coefficient(R).
E= T*R
Let us call E1 the efficiency, when the output beam is parallel to the incident beam, and E2 the efficiency of the one that is perpendicular.

Reflection and Transmission for various materials

We discuss the efficiency for three materials (quartz, Mylar, Kapton) and different thickness versus transmission and reflection coefficients.

An other important parameter is the angle of the plate. Two cases are examined. The first one is small angle case, say 7°, which allows to separate the reflected beam from the incident one in approximately 50 cm . The second one is the Brewster angle (60°), which allows optimising one reflected component.

One needs to know their ordinary and extraordinary index and absorption coefficients at 118 microns:

	O index	O absorption (cm-1)	X index	X absorption (cm-1)	Reference
Natural Quartz	2.1204	.63	2.1694	.47	(1)
Mylar	1.7	40	1.7	40	(2)
Kapton	1.793	8.3	1.793	8.3	(2)

The values come from two references
Ref 1 : Veron : Submillimeter Interferometry of high density plasmas, in Infrared and millimetre waves, vol 2 , edited by K Button ,Academic press 1979
Ref 2 : Applied Optics June 1975 Vol 14 N°6 p 1335

Then one can calculate transmission and reflection of a parallel face plate versus its thickness and the angle of incidence. Private electromagnetic matlab code is used, but it can be understood in studying ref 3
Ref 3 : Veron , appl optics 1986 vol 25 n°5 p621

The codes have been tested a lot of times and it appears that they fit very well the experimental tests .

Results

Case A: incident beam parallel to the incident plane and crossing the plate first.

Plate angle (degree)	7					60				
Output beam polarisation	Parallel to the incident plan			Perp.		Parallel to the incident plan			Perp.	
	T	R	E1	R	E2	T	R	E1	R	E2
Mylar 18 μm	.721	.219	.163	.226	.158		0			
Kapton 25 μm	.829	.151	.125	.156	.126		0			
Kapton 50 μm	.703	.263	**.185**	.270	**.190**		0			
Quartz 2012 μm	.736	.137	.101	.397	.292		0			
Quartz 2423 μm	.532	.357	**.190**	.392	**.209**		0			

Case B : incident beam perpendicular to the incident plan and crossing the plate first.

Plate angle (degree)	7					60				
Output beam polarisation	Parallel to the incident plan			Perp.		Parallel to the incident plan			Perp.	
	T	R	E1	R	E2	T	R	E1	R	E2
Mylar 18 μm	.715	.219	.156	.226	.161		0			
Kapton 25 μm	.825	.151	.125	.156	.129		0			
Kapton 50 μm	.695	.263	**.185**	.270	**.188**		0			
Quartz 2012 μm	.534	.137	.07	.397	.212		0			
Quartz 2423 μm	.526	.357	**.188**	.392	**.206**		0			

Case C incident beam perpendicular to the incident plan and reflecting the plate first.

Plate angle (degree)	7					60				
Output beam polarisation	Parallel to the incident plan			Perp.		Parallel to the incident plan			Perp.	
	R	T	E1	T	E2	R	T	E1	T	E2
Mylar 18 μm	.226	.721	.163	.715	.161	.585	.920	.538	.36	.211
Kapton 25 μm	.156	.829	.130	.825	.129	.595	.976	**.581**	.392	**.233**
Kapton 50 μm	.270	.703	**.190**	.695	**.188**	.569	.953	.543	.395	.225
Quartz 2012 μm	.397	.736	**.292**	.534	**.212**	.740	.857	.634	.213	.157
Quartz 2423 μm	.392	.532	.209	.523	.205	.611	.843	**.515**	.306	**.187**

Case D: incident beam parallel to the incident plane and crossing the plate first.

Plate angle (degree)	7					60				
Output beam polarisation	Parallel to the incident plan			Perp.		Parallel to the incident plan			Perp.	
	R	T	E1	T	E2	R	T	E1	T	E2
Mylar 18 μm	.219	.721	.158	.715	.156	0				
Kapton 25 μm	.151	.829	.125	.825	.125	0				
Kapton 50 μm	.263	.703	**.185**	.693	**.183**	0				
Quartz 2012 μm	.137	.736	.100	.534	.07	0				
Quartz 2423 μm	.357	.532	**.19**	.526	**.188**	0				

Discussion:

- One can see that the efficiency E of a 50 micron Kapton plate is very similar to the one of an optimised natural quartz plate. The expected efficiency always turns around 20%, excepted one case in C where one efficiency reaches 30 and 60%.

-This efficiency seems to be good enough for the diagnostic. Especially if we consider that the probe beam will be mixed with a frequency shifted beam. Thus, on the detector, the signal will be proportional to the product of the two beam mixed amplitudes. As the calculated reflection, transmission and efficiency terms are intensity parameters, the decrease, due to the plate, on the detector will be proportional to the square of the efficiency E. That means a decrease of only 55% on the detector signal.

-The choice of material:

Kapton is a very easy material to use. The visible reflection coefficient of an alignment beam is good enough. The surface quality is also good enough for visible alignment. The Infrared reflection is not very sensitive to a change of the incident angle. It is inexpensive. It can be sensitive to phonic perturbations. Thus the plate boxes must be isolated from any noise source.

- Mylar is less good in term of efficiency, although quite similar, and very cheap.
- Natural quartz is quite expensive but good in efficiency. As the plates are thick, there are two disadvantages. One is that the reflection coefficient changes very fast versus the incident angle. If the following mirrors are too near the plates, some errors of alignments can occur, due to the change of reflectivity versus the angle. The other problem is that a visible beam is reflected on the two interfaces of the plates and a double beam is created, which can lead to mistakes.
-

-Small or Brewster angle.

The efficiency of a Brewster angle is better than the small angle, at least, for the polarisation component which has turned because of the Faraday effect: 58% instead of 20 %

The disadvantages of this configuration are: If no calibration system is settled between the Corner cube and the plate (remember that half wavelength plates cannot be used. Only rotating and removable grids could be used for calibration) one has to correct by soft the measured rotation of polarisation, in taking into account the reflection or transmission coefficients. We have shown (SOFT 2000) that errors on the angle of the plate are far less important when the angle of the plate is small, because, in this configuration, the two coefficients are very similar)

Conclusion : It appears that the gain of power in the Brewster configuration is not worth

-Crossing first the plate or reflection first.

In term of efficiency , it is very similar. The advantage of crossing first is that the incoming infrared (or visible) beam on the CC is stronger in this configuration and will be easier to measure with intermediate detectors.

- Incident polarisation : Nearly no effect. May be it is better to have the strongest reflection coefficient on the polarisation component that has rotated.